

Development of a gel-based electrolyte for determination of heavy metals using  
smartphone



A Thesis Submitted in Partial Fulfillment of the Requirements  
for the Degree of Master of Science in Chemistry  
Department of Chemistry  
Faculty Of Science  
Chulalongkorn University  
Academic Year 2023

การพัฒนาเจลอิเล็กโทรไลต์สำหรับการตรวจวัดโลหะหนักโดยใช้สมาร์ทโฟน



วิทยานิพนธ์นี้เป็นส่วนหนึ่งของการศึกษาตามหลักสูตรปริญญาวิทยาศาสตรมหาบัณฑิต

สาขาวิชาเคมี ภาควิชาเคมี

คณะวิทยาศาสตร์ จุฬาลงกรณ์มหาวิทยาลัย

ปีการศึกษา 2566

Thesis Title	Development of a gel-based electrolyte for determination of heavy metals using smartphone
By	Miss Nuntanuch Lersanantasil
Field of Study	Chemistry
Thesis Advisor	Associate Professor Dr. NARONG PRAPHAIRAKSIT, Ph.D.
Thesis Co Advisor	Professor Dr. ORAWON CHAILAPAKUL, Ph.D.

---

Accepted by the FACULTY OF SCIENCE, Chulalongkorn University in Partial Fulfillment of the Requirement for the Master of Science

----- Dean of the FACULTY OF SCIENCE  
( )

THESIS COMMITTEE

----- Chairman  
(Professor Dr. PAITON RASHATASAKHON, Ph.D.)  
----- Thesis Advisor  
(Associate Professor Dr. NARONG PRAPHAIRAKSIT, Ph.D.)  
----- Thesis Co-Advisor  
(Professor Dr. ORAWON CHAILAPAKUL, Ph.D.)  
----- Examiner  
(Associate Professor Dr. NATAYA NGAMROJANAVANICH,  
Ph.D.)

นันทน์ เลิศอนันต์สิทธิ์ : การพัฒนาเจลอิเล็กโทรไลต์สำหรับการตรวจวัดโลหะหนักโดยใช้สมาร์ทโฟน. ( Development of a gel-based electrolyte for determination of heavy metals using smartphone) อ.ที่ปรึกษาหลัก : รศ. ดร.ณรงค์ ประไพรัชสิทธิ์, อ.ที่ปรึกษาร่วม : ศ. ดร.อรรวรรณ ชัยลภากุล

ในวิทยานิพนธ์เรื่องนี้ได้นำเสนออุปกรณ์พกพาโดยใช้เจลอิเล็กโทรไลต์สำหรับการตรวจวัดโลหะแคดเมียม และตะกั่วพร้อมๆกันในภาคสนาม ซึ่งเทคนิคนี้เป็นสารโพลีเมอร์จากธรรมชาติที่ถูกนำมาใช้เป็นสารตัวกลางในการขนส่งสารเคมี เนื่องจากคุณสมบัติของเทคนิคสามารถย่อยสลายได้ทางชีวภาพและสามารถละลายได้อย่างรวดเร็ว โดยเทคนิคดีฟเฟอเรนเชียลพัลส์โวลแทมเมทรีถูกนำมาใช้ในการตรวจวัดสัญญาณทางเคมีไฟฟ้าของสารละลายโลหะหนักแคดเมียมและตะกั่วที่ถูกหดยดลงบนเทคนิคเจลอิเล็กโทรไลต์ ในการดัดแปลงขั้วไฟฟ้ากราฟีนแบบพิมพ์สกรีนใช้โลหะผสมสองชนิดคือพลวงและบิสมัทบนหน้าขั้วไฟฟ้าโดยการใช้วิธีสองวิธี คือการดัดแปลงขณะตรวจวัดและการผสมบิสมัทขนาดนาโนกับหมึกกราฟีนของขั้วไฟฟ้าอิเล็กโทรดก่อนการตรวจวัดเพื่อเพิ่มสัญญาณของตัวตรวจวัด จากผลการทดลองแสดงให้เห็นว่าเจลอิเล็กโทรไลต์ที่ถูกพัฒนาขึ้นมีความสามารถในการแสดงสัญญาณของกระแสไฟฟ้าที่มีลักษณะที่คมชัด และมีความแตกต่างแยกกันได้ดีชัดเจน โดยให้ความสัมพันธ์เชิงเส้นตรงกับความเข้มข้นของโลหะแคดเมียมและตะกั่วด้วยขีดจำกัดต่ำสุดของการตรวจวัดอยู่ที่ 50.98 นาโนกรัมต่อมิลลิลิตรสำหรับแคดเมียม และ 40.80 นาโนกรัมต่อมิลลิลิตรสำหรับตะกั่ว ความสามารถในการตรวจวัดซ้ำอ้างอิงโดยค่าส่วนเบี่ยงเบนมาตรฐานสัมพัทธ์ซึ่งพบว่ามีค่าน้อยกว่า 10.4% ซึ่งใช้จำนวนการตรวจวัดเท่ากับ 10 ครั้งโดยประกอบการใช้กับเครื่องให้ศักย์ไฟฟ้าที่มีการเชื่อมต่อข้อมูลแบบไร้สาย สุดท้ายนี้ตัวรับสัญญาณที่ประสบผลสำเร็จนี้ได้มีการนำไปประยุกต์ใช้ในการวิเคราะห์และตรวจหาปริมาณโลหะแคดเมียมและตะกั่วในตัวอย่างเครื่องดื่มที่มีการผสมกัน ซึ่งค่าร้อยละการกลับคืนที่ได้จากการทดลองอยู่ในช่วงที่ยอมรับได้ซึ่งมีค่าเท่ากับ 80-110% นอกจากนี้แพลตฟอร์มที่ถูกออกแบบใหม่แสดงให้เห็นถึงประโยชน์อีกมากมายอย่างเช่น การใช้สารตัวอย่างในปริมาณน้อยในระดับไมโครลิตร ราคาถูก ไม่มีความต้องการที่ต้องเตรียมสารตัวอย่าง และสามารถย่อยสลายได้ทางชีวภาพ

สาขาวิชา เคมี

ลายมือชื่อนิสิต .....

ปีการศึกษา 2566

ลายมือชื่อ อ.ที่ปรึกษาหลัก .....

ลายมือชื่อ อ.ที่ปรึกษาร่วม .....

# # 6470104223 : MAJOR CHEMISTRY

KEYWORD: polymer electrolyte, Bio-based polymer, paper-based analytical devices, mobile phone, near field communication

Nuntanuch Lersanantasi : Development of a gel-based electrolyte for determination of heavy metals using smartphone. Advisor: Assoc. Prof. Dr. NARONG PRAPHAIRAKSIT, Ph.D. Co-advisor: Prof. Dr. ORAWON CHAILAPAKUL, Ph.D.

Herein, a portable electrochemical device using biopolymeric gel-based electrolyte for the on-field simultaneous determination of Cd(II) and Pb(II) is presented. Pectin, a natural polymer, was used as a chemical delivery medium due to its biodegradation and fast-dissolving properties. Differential pulse voltammetry (DPV) was used to detect electrochemical signal of Cd(II) and Pb(II) solution dropped on the pectin-based electrolyte platform. The modification of screen-printed graphene electrode with Sb-Bi bimetallic alloy using both in situ and pre-mixed method was able to enhance the sensitivity of the sensor. The experimental results demonstrated that the developed gel-based electrolyte was capable of generating sharp and well-defined current signals, achieving the low detection limits of 50.98 ng mL<sup>-1</sup> for Cd(II) and 40.80 ng mL<sup>-1</sup> for Pb(II). The reproducibility, as indicated by the relative standard deviation was found to be less than 10.4% (n=10), when coupled with the NFC potentiostat. Lastly, the obtained sensor was utilized to analyze and quantify the two metals in various samples of cannabis-infused drinking water. The recoveries were obtained within the acceptable range of 80-110%. Moreover, the newly designed platform exhibited several advantages, such as, small sample volume (μL), low-cost, no sample preparation requirements, and biodegradability.

Field of Study: Chemistry

Academic Year: 2023

Student's Signature .....

Advisor's Signature .....

Co-advisor's Signature .....

## ACKNOWLEDGEMENTS

This dissertation would not have been possible without the support of these people. First and foremost, I would like to express my deepest appreciation to my advisor and my co-advisor, Associate Professor Dr. Narong Praphairaksit, and Professor Dr. Orawon Chailapakul, for kind support, encouragement and guidance throughout my years of study. Additionally, I would like to thank my thesis examination committee, Professor Dr. Paitoon Rashatasakhon, Associate Professor Dr. Nattaya Ngamrojavanich, and Associate Professor Dr. Weena Siangproh for their helpful comments and invaluable advice in this dissertation.

I would like to acknowledge the financial and facilities support from National Research Council of Thailand (NRCT), Electrochemistry and Optical Spectroscopy Center of Excellence (EOSCE), Department of Chemistry, Faculty of Science, Chulalongkorn University.

Lastly, I sincerely appreciate my family and my friends for their unfailing support and continuous encouragement through the process of researching and writing this dissertation. This accomplishment would not be possible without them. Thank you.

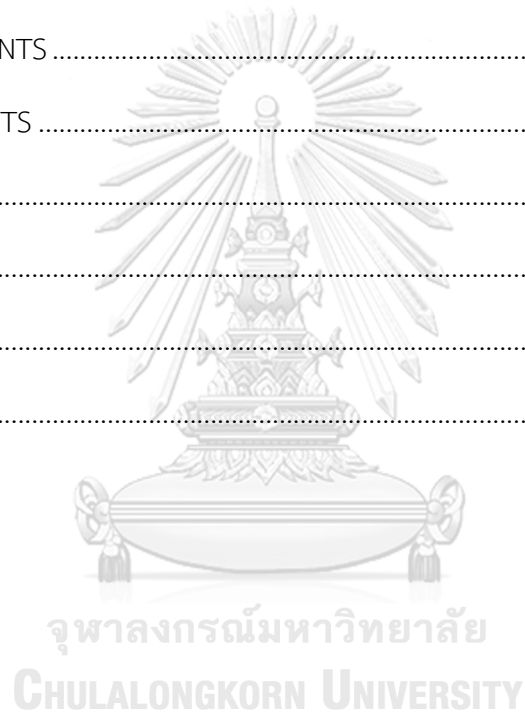


จุฬาลงกรณ์มหาวิทยาลัย  
CHULALONGKORN UNIVERSITY

Nuntanuch Lersanantasil

## TABLE OF CONTENTS

	Page
.....	iii
ABSTRACT (THAI) .....	iii
.....	iv
ABSTRACT (ENGLISH) .....	iv
ACKNOWLEDGEMENTS .....	v
TABLE OF CONTENTS .....	vi
LIST OF TABLES.....	vii
LIST OF FIGURES.....	viii
REFERENCES.....	51
VITA.....	59



## LIST OF TABLES

	<b>Page</b>
Table 1 List of instruments and apparatus. ....	22
Table 2 List of chemicals and materials. ....	23
Table 3 The operating parameters of ICP-OES. ....	27
Table 4 Comparison of the analytical performance of the Sb-Bi/BiNP/SPGE using pectin-based electrolyte with other works for heavy metals determination using electrochemical sensors. ....	45
Table 5 Recovery tests of the proposed sensor and conventional method for the simultaneous determination of Cd(II) in cannabis-infused drinking water samples (n = 3). ....	48
Table 6 Recovery tests of the proposed sensor and conventional method for the simultaneous determination of Pb(II) in cannabis-infused drinking water samples (n = 3). ....	49





## LIST OF FIGURES

	Page
Figure 1 The heavy metal contamination in groundwater and associated ecological and human health risks of a geologically and anthropogenically. Adapted with permission from ref (17) Copyright 2020 Science of the Total Environment.....	4
Figure 2 The family tree of interfacial electrochemical techniques (22).....	7
Figure 3 (a) Typical potential variation and (b) the shape of the I–E curve in the popular technique known as cyclic voltammetry (21).....	9
Figure 4 (a) differential pulse waveform and (b) differential pulse voltammogram where $\Delta i_p$ is the difference current between two points (21).....	10
Figure 5 Screen-printed graphene paste electrode (SPGE) (28).....	13
Figure 6 Classification of electrolytes commonly used (31).....	15
Figure 7 NFC Modes of Communication (34).....	17
Figure 8 Examples of NFC Communication Modes (34).....	17
Figure 9 (a) Photograph of a ready-to-use toolbox developed for on-field analysis and (b) the welcome interface and example of the detection data displayed on the smartphone application (36).....	18
Figure 10 The schematic of (a) gel-based electrolyte pad, (b) screen-printed graphene electrode, and (c) sample barrier configurations. ....	24
Figure 11 Scheme of the gel-based electrolyte platform and its operation.....	26
Figure 12 SEM images of a bare filter paper (A), and biopolymeric gel-based electrolyte covered filter paper (B-C).....	29
Figure 13 Elemental analysis of the gel-based electrolyte pad by energy dispersive X-ray fluorescence (EDXRF). ....	29

Figure 14 DPV curves (A) and anodic currents (B) of blank solution (0.1 M HCl) and 0.5 $\mu\text{g mL}^{-1}$ Cd(II) and Pb(II) in 0.1 M HCl (liquid electrolyte platform).....	31
Figure 15 DPV of blank solution and 1 ppm Cd(II) and Pb(II) containing modified gel-based electrolyte on Bi/BiNP/SPGE.....	33
Figure 16 Effect of optimized experimental parameters for the determination of Cd(II) and Pb(II) such as DPV curve (A) and anodic currents (B) of gap thickness of the device. ....	34
Figure 17 Effect of biopolymers used as gel-based electrolyte for the determination of Cd(II) and Pb(II).....	35
Figure 18 Effect of various pH of gel-based electrolyte for the determination of Cd(II) and Pb(II). ....	36
Figure 19 Effect of optimized type of supporting electrolyte for the determination of Cd(II) and Pb(II).....	37
Figure 20 Effect of optimized various concentration of supporting electrolyte for the determination of Cd(II) and Pb(II).....	38
Figure 21 Effect of pectin content for the determination of Cd(II) and Pb(II). ....	39
Figure 22 Effect of the Sb/Bi concentration ratio for the determination of Cd(II) and Pb(II).....	40
Figure 23 Effect of concentration of BiNP for the determination of Cd(II) and Pb(II). .	41
Figure 24 Effect of deposition potential (A), deposition time (B), amplitude (C) and step potential (D) to the stripping current of 1000 $\text{ng mL}^{-1}$ Cd(II) and Pb(II); the signals are shown as means of the measured values (n=3).....	42
Figure 25 (A) DPVs of blank solution (milli-Q water), Cd(II), and Pb(II) at concentrations of 0-1500 $\text{ng mL}^{-1}$ using gel-based electrolyte on a Sb-Bi modified screen-printed electrode. (B) A linear relationship between the oxidative currents and concentrations of Cd(II) and Pb(II).....	43

- Figure 26 The reproducibility of the Sb-Bi/BiNP/SPGE using pectin-based electrolyte for the determination of 400-1000 ng mL<sup>-1</sup> Cd(II) and Pb(II); the signals are shown as peak height of the measured values (n=10).....44
- Figure 27 Long-term stability of Sb-Bi/BiNP/SPGE using pectin-based electrolyte; Cd(II) 1000 ng mL<sup>-1</sup> and Pb(II) 1000 ng mL<sup>-1</sup> ; the signals are shown as means of the measured values (n=3).....44
- Figure 28 Influence of common ions on the current signal of Cd(II) (a) and Pb(II) (b), ratios are given as m(interferent):m(Cd(II)/Pb(II)); the signals are shown as means of the measured values (n=3).....47



## CHAPTER I

### INTRODUCTION

#### 1.1 Introduction

Cadmium (Cd) and Lead (Pb) are two heavy metals that are commonly exposed to humans through environment, soils and sediments. Both elements can cause many adverse health effects after accumulation in the body such as skeletal and cardiovascular dysfunctions, hepatic and renal damage, and reproductive illness (1). Therefore, Cd and Pb detection method is important in order to avoid the risk of chronic poisoning (2). The conventional methods used for the determination of heavy metals such as atomic absorption spectroscopy (AAS), inductively coupled plasma atomic emission spectroscopy (ICP-AES) (3), and inductively coupled plasma mass spectrometry (ICP-MS) (4), have limitations in terms of high-cost instrument and complicated operation.

Electrochemical methods offer many advantages such as low cost, portability, and high sensitivity (5). Generally, a supporting electrolyte is used in electrochemical analysis for ions balancing between an anode and a cathode of an electrochemical cell. However, the supporting electrolyte solutions still require daily preparation with sample solution before analysis. To address this drawback, a biopolymeric gel-based electrolyte like pectin has been used as a chemical storage because of their biodegradability and non-toxicity (6). Moreover, the attractive properties of Bi(II) and Sb(II) film electrodes provided high sensitivity and well-defined stripping signals of Cd(II) and Pb(II) (7).

Polyvinyl alcohol (PVA) has been frequently used to form a gel-based electrolyte in the field of conductivity and electrochromic devices (8). Recently, PVA gel-based electrolyte was applied for electrochemical detection of herbicide by

Charoenkitamorn et al. PVA was dissolved in a DMSO:water media to create the PVA gel-electrolyte.  $\text{LiClO}_4$  was introduced as a supporting electrolyte to PVA gel-based after cooling to room temperature (9). However, the PVA conditions require a long time to transfer analyte to the electrode surface and a very toxic substance for the gel electrolyte formation. Other gel-based electrolyte materials, such as hydroxypropyl cellulose-based (HPC) (10), pectin-based polymers (11) have also been employed for safer operation. Pectin, as a biopolymer, is widely recognized as an effective biomaterial for producing the edible films and coatings, due to their mechanical properties, biocompatibility, biodegradability, and non-toxicity. Pectin is utilized as a delivery system for the controlled release of various medications (12). It was found that pectin can form complexes with a variety of metallic species, making it worthy to use as a heavy metal adsorbent (13). With such a property, pectin can hence be applied for the determination of heavy metal. Additionally, these materials offer the capability to modify the release profile of electrolyte, making them suitable for ready-to-use electrochemical sensor.

In this work, a biopolymeric gel-based electrolyte using a Bi-Sb alloy modified screen-printed electrode was developed for the simultaneous determination of Cd(II), and Pb(II). This platform was coupled with a smartphone-based electrochemical analysis and a near-field communication (NFC) potentiostat card for real-time and on-field testing. Furthermore, the platform on Bi-Sb modified screen-printed electrode could provide sharp and well-defined current signals of both Cd(II) and Pb(II), superior to those obtained with the conventional electrolyte.

## 1.2 Objective of the research

To develop a gel-based electrolyte on a Sb-Bi modified screen-printed electrode for the simultaneous determination of Cd(II) and Pb(II) on a smartphone using wireless technology

### 1.3 Scope of this research

This pectin gel-based electrolyte was integrated with Sb-Bi bimetallic-modified screen-printed graphene electrode as an electrochemical sensor. This sensor will be coupled with smartphone-based electrochemical analysis and near-field communication (NFC) potentiostat card to determine simultaneously Cd(II), and Pb(II) in cannabis drink samples with high sensitivity, accuracy, and ease of use.



## CHAPTER II

### THEORY AND LITERATURE REVIEW

#### 2.1 Heavy metals

Heavy metals such as Cd, Cr, Hg and Pb are generally defined as metals with high density, atomic mass number or atomic weight (14). Cadmium (Cd) and lead (Pb) are ordinary toxic heavy metals in the environment. Cd(II) and Pb(II) are explored through ambient air, drinking water, food, industrial substantial, and consumer production (15). Both elements can cause many health effects after accumulation in the body such as skeletal and cardiovascular dysfunctions, hepatic and renal damage, and reproductive illness. The average lead and cadmium concentrations in groundwater are 44.7  $\mu\text{g/L}$  and 3  $\mu\text{g/L}$ , respectively, which is beyond the desired limits of 10  $\mu\text{g/L}$  and 3  $\mu\text{g/L}$  as recommended by BIS (1991) and WHO (2006), while the ranges for these concentrations are 6.7 to 82.7  $\mu\text{g/L}$  and 0.1 to 5.9  $\mu\text{g/L}$ , respectively (16). Therefore, a highly-sensitive, selective and reliable method is critically needed to monitor and control the concentration of Cd(II) and Pb(II).

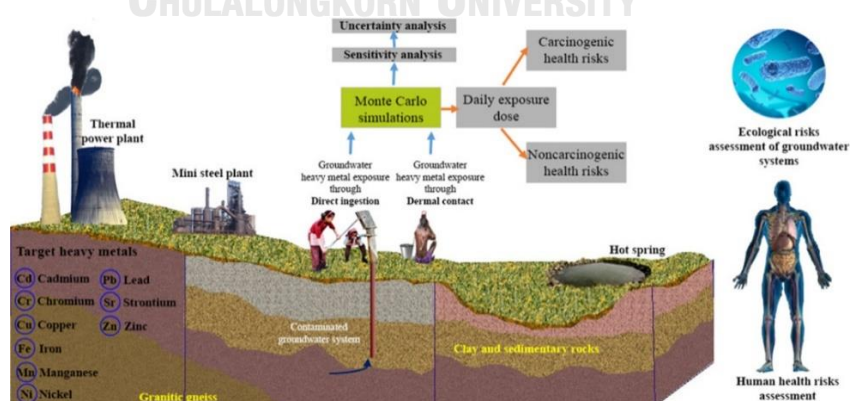


**Figure 1** The heavy metal contamination in groundwater and associated ecological and human health risks of a geologically and anthropogenically. Adapted with permission from ref (17) Copyright 2020 Science of the Total Environment.

Currently, the conventional methods for Cd(II) and Pb(II) detection consist of atomic absorption spectroscopy (AAS) (18), inductively coupled plasma atomic emission spectroscopy (ICP-AES) (19), and inductively coupled plasma mass spectrometry (ICP-MS) (20). However, these analytical techniques all require expensive instrument and high operating cost. Additionally, these methods have some drawbacks such as bulky and sophisticated instruments that are unsuitable for on-field analysis. To improve the throughput of such analysis, it is critically necessary to develop a low-cost, quick, and simple sensor for heavy metal detection using electrochemical detection.

## 2.2 Electrochemical detection

Electrochemical detection is often used the first option for miniature sensing devices due to its rapid processing, high sensitivity, and low power need. The electrochemical detection is widely employed in a variety of applications and is based on the measurement of electrical values including current, potential, or charge produced by the electron transfer of target analyte at the electrode/electrolyte interface. Voltammetry is one of the electrochemical methods that primarily depends on the investigation of the charge-transfer or electron transfer process at the electrode surface, where the current response is observed after applying the potential.

### 2.2.1 Faradaic and non-faradaic process

Two specific types of reactions occur at the electrode surface (21). Charges (electrons) are transferred across the electrode-solution interface in the first step. The reduction or oxidation that results from this electron transport is referred to as a faradaic reaction. The external current that travels via the electrode-electrolyte contact as a result of the adsorption and desorption processes is what drives the second process. Additionally, non-faradaic events, which occur when the voltage or composition of the solution changes, can cause the structure of the electrode-solution



interface to alter. Background current is the term used to describe the non-faradaic current.

### 2.2.2 Mass transfer

For electrochemical processes, transport of significant molecules from the bulk solution to the electrode surface might contribute to the redox reaction at the electrode boundary. This driving force, sometimes referred to as the mass transfer process, significantly affects both the kinetics of electron transfer and the rate of the electrochemical reaction (21). Theoretically, there are three different kinds of mass transportation behaviour:

1) Migration is the movement of charged species when an electric field (an electrical potential gradient) is present.

2) Diffusion is the transfer of species from a high-concentration area to a low-concentration area while being influenced by a concentration gradient.

3) Convection is the movement of species while they are being stirred or subjected to hydrodynamic forces. The characterization of stationary areas, laminar flow, and turbulent flow can be done via forced convection.

The Nernst-Planck equation, which governs the mass transfer to an electrode in one dimension along the x-axis, is expressed as

$$J_i(x) = -D_i \frac{\partial C_i(x)}{\partial x} - \frac{z_i F}{RT} D_i C_i \frac{\partial \phi(x)}{\partial x} + C_i \mathbf{V}(x)$$

Where  $J_i(x)$  represents the flux of species  $i$  ( $\text{mol s}^{-1} \text{cm}^{-2}$ ) at distance  $x$  from the surface,  $D_i$  is the diffusion coefficient ( $\text{cm}^2/\text{s}$ ),  $\partial C_i(x)/\partial(x)$  represents the concentration gradient at distance  $x$ ,  $\partial \Phi(x)/\partial(x)$  represents the potential gradient, and  $z_i$  and  $C_i$  represent the charge (dimensionless) and concentration ( $\text{mol cm}^{-3}$ ) of species  $i$ , respectively,  $\mathbf{V}(x)$  is the velocity ( $\text{cm/s}$ ) which a volume element in solution moves

along the axis. The three terms on the right-hand side, which stand for the flux contributions of convection, migration, and diffusion, respectively.

### 2.2.3 Electrochemical method

Electrochemical methods are a class of techniques in analytical chemistry which generally involve measuring how an electrochemical cell with an ion-conducting phase, called the electrolyte, reacts to the application of an electric input through electrodes immersed in the electrolyte. The electrochemical methods studied an analyte by measuring the potential (volts) and/or current (amperes) in an electrochemical cell containing the analyte. Depending on which features of the cell are manipulated and which are measured, these techniques can be divided into several categories. Potentiometry, which measures the difference between electrode potentials, amperometry, coulometry, which records the charge passed over a given period, and voltammetry, which measures the cell's current while actively modifying the cell's potential.

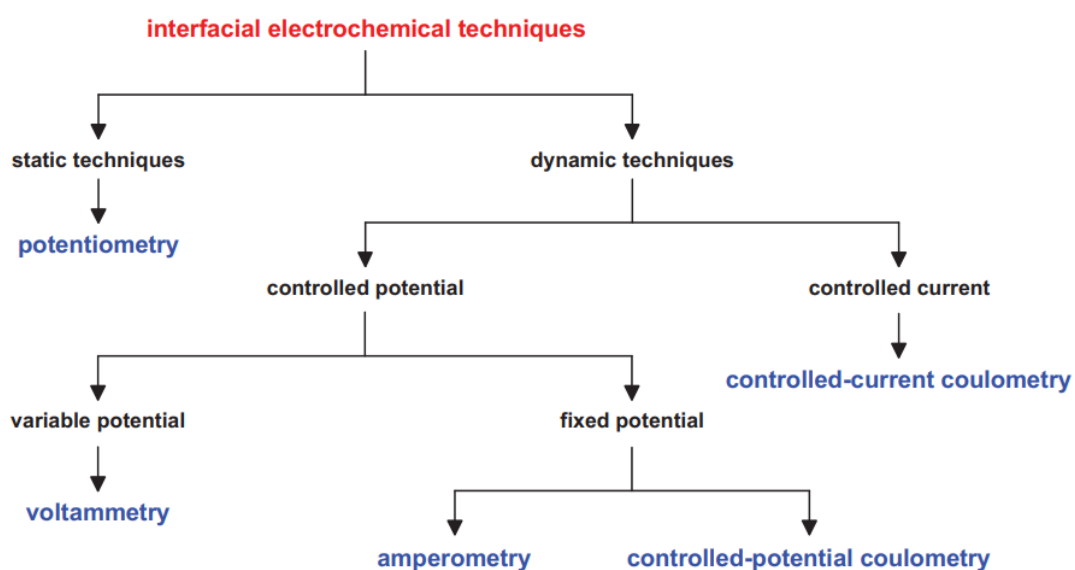


Figure 2 The family tree of interfacial electrochemical techniques (22)

### 2.2.3.1 Voltammetry

Voltammetric methods are electrochemical techniques that rely on the measurement of current as a function of applied voltage. These methods are based on the measurement of current in an electrochemical cell under fully polarized concentration conditions, where the rate of analyte mass transfer to an electrode's surface controls how quickly analytes can be reduced or oxidized. Voltammogram is the name given to the current vs. potential plot produced by this technique. Depending on the applied potential waveforms, various voltammetry techniques are employed in electrochemical analysis, including cyclic voltammetry, polarography, linear sweep voltammetry, staircase voltammetry, normal pulse voltammetry, differential pulse voltammetry, square wave voltammetry, anodic stripping voltammetry and cathodic stripping voltammetry, as well as adsorptive stripping voltammetry.

#### 2.2.3.1.1 Cyclic voltammetry

Cyclic voltammetry (CV) is the most common and popular technique. The redox reaction process (oxidation-reduction reaction) of the target analytes is often investigated using the most prevalent and well-liked electrochemical detection technique, known as CV. Additionally, CV is used to investigate the characterization, electrochemical characteristics, and chemical reactions of intriguing analytes that are started by electron transfer. An electrolyte solution with an electroactive species is subjected to a triangle potential waveform (Figure 3a). In order to force a reduction reaction of an electroactive species, the potential is scanned from a negative direction, and the cathodic peak is subsequently produced. On the other hand, the WE surface will experience the oxidation reaction if the potential is scanned back in a positive direction. As shown in Figure 3b, the voltammograms are shown between the current response (i) and potential (E) and represent the findings of the CV approach.

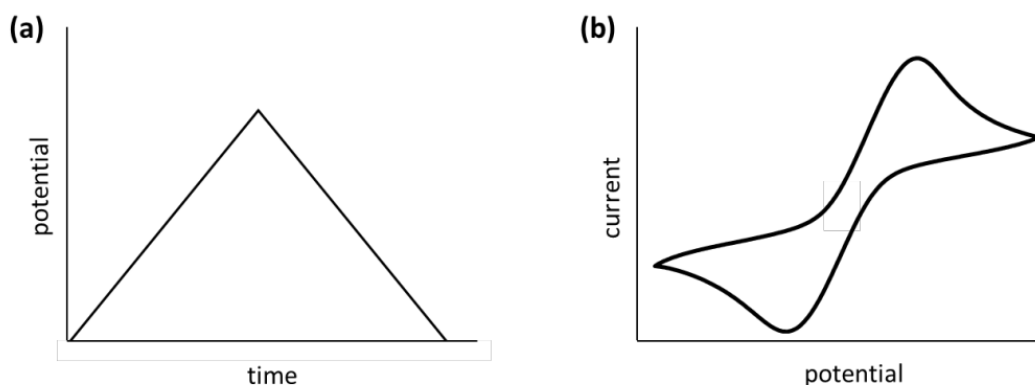


**Figure 3** (a) Typical potential variation and (b) the shape of the I-E curve in the popular technique known as cyclic voltammetry (21).

The Randles-Sevcik equation can be used to describe the reversible system at 25°C where the generated peak current ( $I_p$ ) from CV is proportional to the concentration of the target analyte.

$$I_p = (2.69 \times 10^5) n^{\frac{3}{2}} A F C D^{\frac{1}{2}} v^{\frac{1}{2}}$$

Where A is the effective electrode area ( $\text{cm}^2$ ), F is the faraday constant ( $\text{C mol}^{-1}$ ), C is the concentration ( $\text{mol cm}^{-3}$ ), D is the diffusion coefficient ( $\text{cm}^2 \text{s}^{-1}$ ) and v is the scan rate ( $\text{V s}^{-1}$ ), n is the number of electrons. The peak position on the potential axis ( $E_p$ ) is related to the potential of analyte in reaction. The formal potential in the reversible system is centered between  $E_{p,a}$  and  $E_{p,c}$ .

$$E^\circ = \frac{E_{p,c} + E_{p,a}}{2}$$

The peak separation between the peak potentials ( $E_p$ , mV) is provided by

$$\Delta E_p = E_{p,a} - E_{p,c} = \frac{59}{n}$$

By separating the cathodic and anodic peak potentials, it is possible to calculate how many electrons were transported during the reduction-oxidation reaction. Despite

this, due to its limited sensitivity, the CV technique is typically utilized for the qualitative determination of electroactive species.

### 2.2.3.1.2 Differential pulse voltammetry

Differential pulse voltammetry (DPV) is one of the voltametric measurements that is used to create a derivative of linear scan voltammetry or staircase voltammetry with a series of voltage pulses superimposed over the potential linear scan. This method involves checking the current before each proposed modification. The impact of the charging current can be significantly reduced by taking the current samples prior to the potential change (21). The applied potential in DPV is typically swept with a succession of a pulse (Figure 4a), and the current response is measured at two-point. Before applying the pulse at location 1, current ( $i_1$ ) is measured first (before administering the pulse, time 1). At the end of the pulse, when the charging current has decayed ( $t_2$ ), the current ( $i_2$ ) is then measured once more. In Figure 4b, the applied potential is displayed against the difference in the current response between the two sites ( $\Delta i = i_1 - i_2$ ).

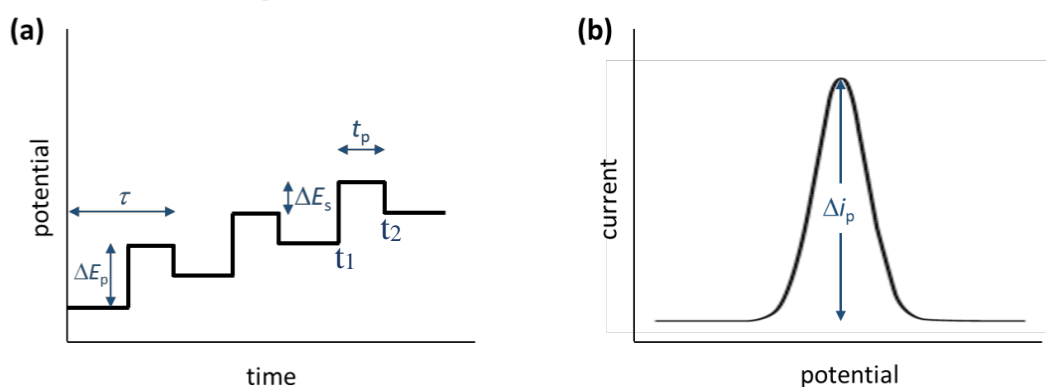


**Figure 4** (a) differential pulse waveform and (b) differential pulse voltammogram where  $\Delta i_p$  is the difference current between two points (21).

Especially, the differential pulse anodic stripping voltammetry (DPASV) has been employed for the determination of trace elements because DPASV has excellent sensitivity, the capability of simultaneous multiple elements detection, and simple implementation of the trace metal (23). The DPASV was performed on the common electrode as a glassy carbon electrode (GCE) because it is a convenient and highly sensitive technique for heavy metal detection (24).

### 2.3 Electrochemical cell

An electrochemical cell is a device that produces an electrochemical current using the energy released by a spontaneous redox process (reduction-oxidation reaction). Two conductive electrodes, known as the anode and cathode, make up an electrochemical cell. The electrode where oxidation takes place is called the anode, and the electrode where reduction takes place is called the cathode. In a two-electrode system, which includes a working electrode (WE), and a counter/reference electrode (CE/RE), both of which are used to measure the potential across the complete cell. When the potential is measured against the reference electrode, the potential could be decreased by the resistance of current flowing between the interface of solution and electrode. Therefore, the counter electrode is required to prevent the current from flowing through the reference electrode, which would alter the potential of the reference electrode. As a result, the counter electrode is a secondary electrode that is required to complete the circuit and conduct current in the system. This study made use of a three-electrode setup. The elements of the WE, CE, and RE are the components of this system.

#### 2.3.1 Working electrode

The most crucial part of an electrochemical cell is the working electrode (WE). Target analytes undergo a redox reaction and transfer electrons at the electrode

surface. For long-term stability, good electrochemical inertness, and durability, the WE should be made of inert materials such as platinum, gold, carbon, and mercury. The success of the experiment depends heavily on the WE material selection. Depending on their intended application, the materials used to create WE vary in type, size, and shape. To enhance the performance of paper-based analytical device (PAD), two types of screen-printed graphene electrode (SPGE) are used as WE in this study.

### 2.3.1.1 Screen-printed electrode

Today's technology allows for the simple production of a new type of electrode using screen printing. Different inks, such as carbon, graphene, and graphene oxide, are chosen as conducting materials for screening on substrates like filter paper or plastic (PVC). The various types of ink used for screening affect the analytical detection selectivity and sensitivity. Because of the manufacturing process, they are referred to as screen-printed electrodes. The three-electrode system, namely, a working, counter, and reference electrode, has been miniaturized onto the substrate for a single-use and low-cost device. Alternatively, a screen-printed electrode has been employed to determine a target analyte within a small volume of sample and reagent (25). Moreover, paper-based devices integrated with electrochemical sensor containing electrolytes (26, 27) has been demonstrated as an inexpensive and miniaturized electrochemical sensor.

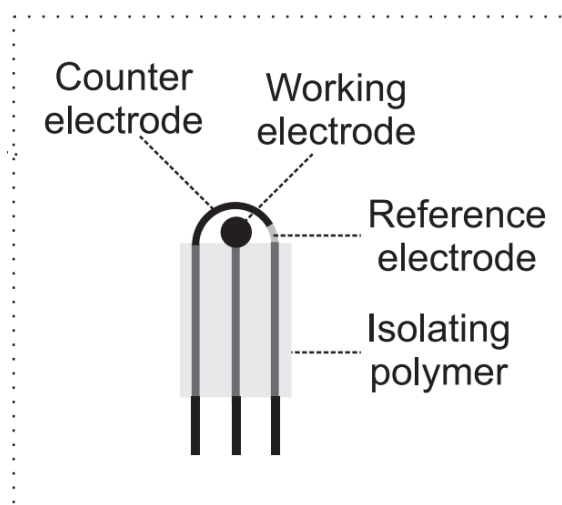


**Figure 5** Screen-printed graphene paste electrode (SPGE) (28)

#### 2.3.1.2 Counter electrode (CE)

The electrode in an electrochemical cell that completes the current circuit is known as the counter electrode (CE) or auxiliary electrode (AE). This electrode is made of inert substances including platinum, gold nanoparticles, graphite, glassy carbon, and others. Because CE can operate as an electron source and does not restrict the kinetics of an electrochemical process during electrochemical measurement, its surface area should be greater than WE's.

#### 2.3.1.3 Reference electrode (RE)

To determine the potential of WE without passing current through the electrochemical cell, the reference electrode (RE) is used. The RE must offer a consistent, recognizable, and well-defined electrochemical potential. Ag/AgCl was chosen as the RE in an electrochemical cell for this study.

#### 2.3.1.4 Supporting electrolyte

Another key component of the electrochemical system is the supporting electrolyte. They are soluble chemicals whose ions have a high ionic mobility which



enables them to migrate and carry charge as a result of the electric field produced by the potential difference (29). This maximizes migratory transport and creates a diffusive control within the cell. All of this is due to the fact that the diffusion current, which is related to concentration in voltammetry, introduces deviations from the theoretical equations governing the process. This, in turn, causes the voltammetric quantification method to lose accuracy and precision in real-world applications. The supporting electrolyte solution is used for ions balancing between an anode and a cathode of electrochemical cell. Additionally, electrolytes in a solvent can be categorized based on the solvents in which they are dissolved or based on their properties in the neat state.

#### **2.3.1.4.1 Liquid electrolyte**

##### **2.3.1.4.1.1 Aqueous electrolyte solutions**

Aqueous electrolyte is a liquid electrolyte that has been used in various research. Electrolytes in water is the most significant class. Seawater, hard water, and biological solutions like intra- and extracellular water are a few examples. In aqueous systems, ions are everywhere, even when they are undesired impurities that are only present in very minute concentrations. In spite of this, they are nevertheless able to affect phase equilibria due to their robust interactions with water molecules, other dipoles, and ions (30).

##### **2.3.1.4.1.2 Nonaqueous electrolyte solutions**

The use of nonaqueous electrolyte solutions is directly related to the development of contemporary energy-storing devices (batteries and capacitors). One well-known example is lithium tetrafluoroborate in propylene carbonate. Other areas of electrochemistry, such as electroplating, electrodeposition, or electrochemistry, likewise heavily rely on nonaqueous solutions.

### 2.3.1.4.2 Solid-state electrolyte

Recently, there has been a lot of interest in solid-state electrolyte due to the quick development of flexible supercapacitors. Solid-state electrolytes, in particular, provide a number of benefits over liquid electrolytes, including no electrolyte leakage, easy handling, lightweight, stable, and adaptable structural design. This electrolyte was created using solid polymer electrolytes, gel polymer electrolytes, and polyelectrolytes, which are all three different types of polymer electrolytes. However, the gel polymer, which has better ionic conductivity than other solid-state electrolytes, dominates the solid-state electrolyte-based supercapacitor. This is as a result of them having a liquid phase. Gel polymer electrolyte, sometimes referred to as hydrogel, is made up of a conducting salt or aqueous electrolytes that have been dissolved in a solvent to give mobile ions, such as PVA, PEG,  $\text{H}_2\text{SO}_4$ , KOH, or KCl. However, the low working temperature and very weak mechanical strength of hydrogel electrolytes are their major drawbacks (31).

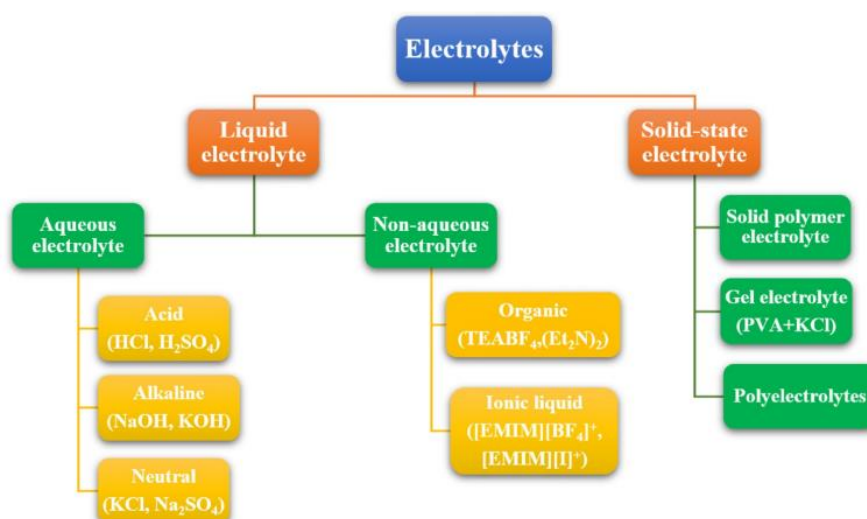


**Figure 6** Classification of electrolytes commonly used (31)

Liquid electrolyte has been used commonly because it is simply prepared in a laboratory. Important properties of liquid electrolytes include their ease of preparation,

high conductivity, low viscosity, and the ability to facilitate effective interfacial wetting between the electrolyte and electrode surfaces (32). However, liquid electrolyte in the system still needs preparation by handling and proficient user on-site.

For in-field testing, the integration of small sensing devices with simplified tools is typically of significant importance. Due to its potent internal sensing function, real-time display, internal data storage, data transfer, and connectivity capabilities, smartphone-based sensing systems have recently been widely developed as portable devices for a wide range of applications (33).

#### **2.4 Near-field communication (NFC)**

Near Field Communication (NFC) is indeed a set of radio transmission standards that enables the exchange of data between electronic devices over short distances. The maximum communication range for NFC is typically about 4 cm or 1.6 inches. NFC operates at 13.56 MHz and uses inductive coupling to establish a connection between devices. Devices can be physically touched or brought close enough to transmit data by this means. Additionally, a tag with an unpowered NFC chip and an NFC device can communicate with one another. To ensure interoperability, the NFC Forum gathers a number of vendors, manufacturers, and service providers. The terms NFC card emulation method, P2P method, and reader/writer method refer to three alternative ways that NFC systems can operate as shown in Fig. 7-8. The NFC behaves like a radio-frequency identification (RFID) system in the first manner. Therefore, it is possible to think of the NFC system in this working mode as an advancement of RFID technology. The P2P mode permits NFC devices to exchange data spontaneously among themselves. The final mode enables tags to be read and written to by NFC devices (34).

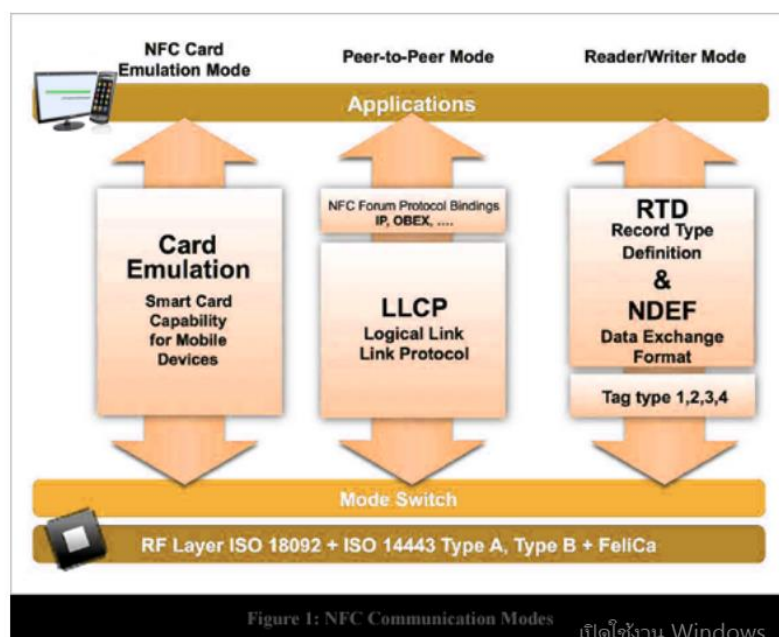
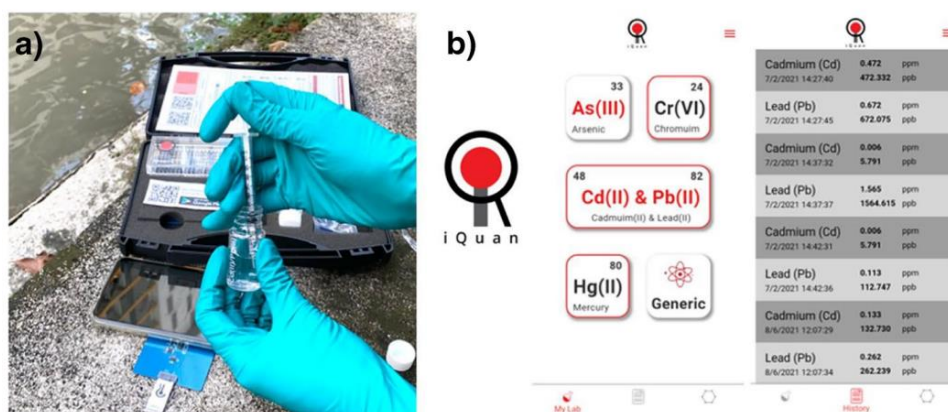


Figure 7 NFC Modes of Communication (34)



Figure 8 Examples of NFC Communication Modes (34)

The electrochemical community is currently very interested in a portable potentiostat for conducting electrochemical measurements. The NFC potentiostat is currently the simplest portable potentiostat available. A wireless communication technology called near-field communication (NFC) creates contactless connections between two suitable devices (35). A tabletop potentiostat's size and cost can be significantly reduced by using a small NFC circuit tag because of the less expensive printed circuit board manufacturing technique. Consequently, the NFC electronic tag will be used to determine the presence of heavy metals (36).



**Figure 9** (a) Photograph of a ready-to-use toolbox developed for on-field analysis and (b) the welcome interface and example of the detection data displayed on the smartphone application (36).

## 2.5 Literature reviews

A gel polymer electrolyte on the electrochemical platform as a ready-to-use device has been a topic of interest because it provides several benefits including no electrolyte leakage, simple handling, light weight, stability, and adaptable structural design as demonstrated by the following works.

(i) In 2020 (9), Charoenkitamorn et al. developed a polyvinyl alcohol (PVA) gel-electrolyte. The preparation of the PVA gel-electrolyte was performed by dissolving PVA in DMSO:water media. After cooling down at room temperature,  $\text{LiClO}_4$  was added as a supporting electrolyte into the PVA gel-based. Then, the prepared PVA gel-based electrolyte was dropped onto the electrode surface. The sensor was used to determine paraquat using differential pulse voltammetry with a detection limit of  $0.31 \mu\text{mol L}^{-1}$ .

(ii) In 2015 (10), Ledwon et al. developed a hydroxypropyl cellulose-based (HPC) gel-based electrolyte on an electrochromic device (ECD). The membrane gel electrolyte was shown a good conductivity, thermal stability, transparency, and

adhesion. The results obtained confirmed that the HPC-based electrolyte is suitable for ECD applications with conductive polymers.

(iii) In 2009 (8), Andrade et al. developed a gel-based electrolyte using pectin as a biodegradable material. The pectin-based gel electrolyte was produced by a plasticization process using glycerol and  $\text{LiClO}_4$ . The pectin-based electrolyte obtained was a transparent film with good ionic conductivity, indicating its compatibility with electrochromic devices.

(iv) A Co-polymer of polyvinyl alcohol (PVA) and carboxymethyl cellulose (CMC) as a film electrolyte was developed for use in a powerful energy storage device (37). The polymer electrolyte was produced by the drop casting method with different ratios between PVA and CMC. The electrochemical performance of PVA/CMC film electrolyte exhibited a good conductivity to be used as an electrochemical storage device.

(v) In 2011 (38), Varshney et al. reviewed a development of a polymer electrolyte using aqueous and nonaqueous-based electrolytes containing a natural polymer. The natural polymer-based electrolyte was presented a good conductivity performance and was used as a synthetic electrolyte for batteries and electrochemical devices.

To enhance the sensitivity of  $\text{Cd(II)}$ , and  $\text{Pb(II)}$  signals for electrochemical detection, the modification of electrode using a variety of materials have been reported.

(i) In 2021 (39), Sun et al. prepared a single nanocomposite electrode and modified electrode using a cationic dyestuff Rhodamine B (RhB). Carboxyl functional groups of RhB exhibited good properties such as water solubility and metal-ligand bonding activity. To modify the electrode, RhB solution was added to reducing graphene solution. Next step, the mixed solution was dispersed and dropped onto the surface of GCE. Moreover, the modified electrode was used to determine  $\text{Pb(II)}$  with high analytical performance in terms of a low detection limit (10 nM) and good linear correlation coefficient (0.9999).

(ii) In 2021 (40), Toghan et al. developed an ethylenediaminetetraacetic acid (EDTA) modified electrode. EDTA was formed on the electrode surface by cyclic voltammetry (CV). This modified electrode was used to determine Cu(II), and Pb(II) using linear sweep voltammetry (LSV). The experimental results presented a linear relationship between Cu(II) and Pb(II) concentration and peak current with a low detection limit of 10.2 and 15.4 nM respectively.

(iii) In 2022 (41), Wang et al. developed a modified electrode using Au-Bi bimetallic nanoparticles as an enhanced sensing platform for simultaneous determination of Pb(II) and Cd(II). First, The obtained Au-Bi bimetallic nanoparticles were mixed with reduced graphene oxide (GO). Then, the solution was placed into UV radiation to obtain rGO-metal nanohybrids. The rGO/Au-Bi nanocomposites modified electrode was used to determine Pb(II) and Cd(II) using differential pulse anodic stripping voltammetry (DPASV). The relationship between response current and the concentrations of Cd(II) and Pb(II) was shown good linearity and the limits of detection of 0.05  $\mu\text{M}$  and 0.02  $\mu\text{M}$  respectively.

(iv) A novel Bi-Sb film modified electrode was reported for trace heavy metals analysis (42). First, The GCE was coated with a Bi or Sb or a combination using the in situ method. A Bi-Sb film electrode (Bi-SbFE) was employed to detect simultaneously Pb(II), Cd(II), and Zn(II). The determination of these metals using Bi-SbFE featured a wide linear concentration ranges, high accuracy, good precision with RSD values less than 20.0%, and low limits of detection (2.5  $\mu\text{g/L}$ , 0.2  $\mu\text{g/L}$ , and 0.2  $\mu\text{g/L}$  for Zn(II), Cd(II), and Pb(II), respectively).

(v) A hollow sphere bismuth oxide doped mesoporous carbon nanocomposite material for detection of Pb(II) and Cd(II) was reported by World health organization (WHO) (43). A mesoporous nanocomposite was successfully fabricated for simultaneous Pb(II) and Cd(II) detection at picomolar levels as a result of its high surface area. This electrode exhibited a very low detection limit of 1.72 pM for Pb(II) and 1.58

pM for Cd(II). Furthermore, the developed electrode was applied to determine Pb(II) and Cd(II) in real water samples. The experimental results were in good agreement with those of the conventional method.

To summarize the above literature review, a biopolymeric gel-based electrolyte for the simultaneous determination of Cd(II), and Pb(II) is concentrated on development. In this work, pectin was designed and applied as a gel-based electrolyte platform for the heavy metals detection for on-field analysis. Moreover, the bimetallic of Sb-Bi was modified on screen-printed graphene electrode using in situ and pre-mixed method to enhance of Cd(II) and Pb(II) sensitivity. Finally, this biopolymeric gel-based electrolyte platform was coupled with smartphone-based electrochemical analysis and near-field communication (NFC) potentiostat card for real-time monitoring of Cd(II) and Pb(II) signals in cannabis drinking samples.



## CHAPTER III

## EXPERIMENTAL

In this chapter, the information of the chemicals and materials used to prepare the gel-based electrolyte platform will be provided, followed by the descriptions of the instruments, the electrochemical measurement process, and sample analysis.

## 3.1 Apparatus

The lists of all instruments used in this work are showed in Table 1

**Table 1** List of instruments and apparatus.

Instruments and apparatus	Suppliers
Field emission scanning electron microscope	JEOL ltd., Japan
Ray6 smart CO <sub>2</sub> Laser-cutter	Neotech Co.,Ltd., Thailand
Screen-printed blocks	Chaiyaboon, Thailand
Analytical balance, Mettler Toledo	Mettler, Switzerland
Micropipette	Eppendorf, Germany
Milli-Q water system (18 M $\Omega$ cm)	Millipore Bedford, USA
Inductively coupled plasma-optical emission spectrometer	iCAP 6500 series, Thermo Scientific, USA
NFC potentiostat	Silicon Craft Technology PLC, Thailand
Motorola One	Motorola
Portable electrochemical reader	Metrohm DropSens, Spain
The printed circuit board	Silicon Craft Technology PLC, Thailand

### 3.2 Chemicals and materials

Table 2 contains a list of all the chemicals and materials utilized in this research. All chemicals used in this work were of analytical grade and were used without any further purification.

**Table 2** List of chemicals and materials.

Chemicals and materials	Suppliers
Transparent film	tesa 62580, Thailand
Double-sided adhesive tape	tesa 4982, Thailand
Whatman #1 filter paper	Sigma Aldrich, USA
Pectin powder from citrus peel	Sigma Aldrich, USA
Graphene inks	Serve Science, Thailand
Silver/silver chloride (Ag/AgCl) inks	Serve Science, Thailand
Acetone	Merck, Germany
Bismuth nanoparticles (BiNPs, 40–60 nm)	Nanostructured & Amorphous Materials, USA
Potassium chloride	Merck, Germany
Standard antimony solution	Merck, Germany
Standard bismuth solution	Merck, Germany
Standard cadmium solution	BDH, Dubai
Standard lead solution	BDH, Dubai

### 3.3 Fabrication of the electrochemical platform utilizing the pectin gel-based electrolyte

#### 3.3.1 Preparation of the pectin gel-based electrolyte

Pectin has been used as a chemical delivery medium owing to its intrinsic biodegradability, environmental benignity, and rapid dissolution attributes.

Consequently, pectin emerged as the preferred electrolyte delivery medium within the realm of electrochemical platforms. There are several steps in the process of making pectin gel-based electrolyte. Firstly, pectin (0.15 g) and KCl (0.02 g) were dissolved into Milli-Q water (9.9 mL). Subsequently, 100  $\mu\text{L}$  of a mixture containing 10  $\text{mg L}^{-1}$  of  $\text{Bi}(\text{NO}_3)_3$  and  $\text{SbCl}_3$  was added into the solution. The mixture was heated and stirred on a hot plate at 60  $^\circ\text{C}$  for 20 minutes, followed by cooling down to room temperature. The filter paper (Whatman #1 filter paper) was cut into a circular shape (diameter = 1.1 cm) using Ray6 smart  $\text{CO}_2$  Laser-cutter as shown in Fig. 10a. Next, 100  $\mu\text{L}$  of the solution was dropped onto the filter paper and left overnight at room temperature to allow solvent evaporation. Finally, the gel-based electrolyte covered on the filter paper was stored in a desiccator until it was ready for use.

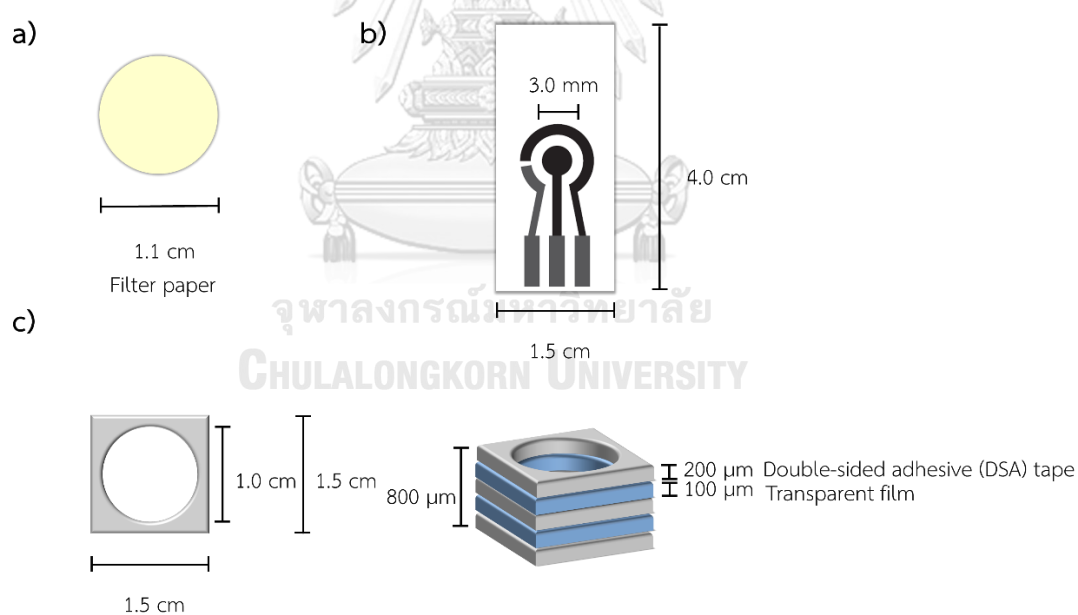


**Figure 10** The schematic of (a) gel-based electrolyte pad, (b) screen-printed graphene electrode, and (c) sample barrier configurations.

### 3.3.2 Design and fabrication of the electrochemical sensor for Cd(II) and Pb(II) detection

The design of the gel-based electrolyte device contains two main parts: the gel-based electrolyte pad and a BiNP-modified SPGE as shown in Fig. 10a-b. The patterns for the device, the gel-based electrolyte pad, three-electrode system, and the gel barrier (transparent film and DSA), were created using Adobe Illustrator program CS6 (Adobe System, Inc.). For the preparation of BiNP-modified SPGE, graphene ink containing 0.5%w/w BiNPs was used to screen-print the working electrode (a circle with a diameter of 3 mm), and counter electrode on a polyvinyl chloride (PVC) substrate (b). The electrodes were kept in an oven at 55 °C for one hour. After that, a reference electrode was screen-printed with Ag/AgCl ink and heated to 55 °C for an hour. For the gel barrier (c), layers of transparent film (TESA 62580, 100 µm thickness) and double-sided adhesive tape (DSA, 200 µm thickness) were cut using a CO<sub>2</sub> laser cutter. The gel barrier was assembled as sample zone in a circular boundary pattern. Lastly, the gel-based electrolyte pad and gel barrier had been piled on top of the BiNP/SPGE. The device was fully assembled and was ready to use prior to the electrochemical measurements.

จุฬาลงกรณ์มหาวิทยาลัย  
CHULALONGKORN UNIVERSITY

### 3.3.3 Operation of the device for the simultaneous measurement of Pb(II) and Cd(II)

The gel-based electrolyte integrated with BiNP-modified SPGE was employed for the detection of Cd(II) and Pb(II). Serial standard dilutions of Cd(II) and Pb(II) were prepared using Milli-Q water and stock standard solutions of the two metals. As shown in Fig. 11, the operating procedures of the electrochemical measurement was depicted. First, the ready-to-use device was placed on the NFC printed circuit board (PCB dimensions: 86 mm x 55 mm x 0.8 mm) in a pin configuration. Subsequently, 100 µL of a mixed solution of Cd(II) and Pb(II) was dropped onto the gel-based electrolyte

pad. The potentiostat was controlled and differential pulse anodic stripping voltammetry (DPASV) was performed using a mobile application (DPV-NE application, version 2.0.0) from Silicon Craft. A deposition potential of  $-1.2$  V vs Ag/AgCl was used for 120 s. The differential pulse voltammograms (DPVs) were recorded using an amplitude of 100 mV, step potential of 20 mV, deposition time of 120 s, and scan rate of 0.1 V/s over a potential range of  $-1.2$  to  $-0.2$  V vs Ag/AgCl.

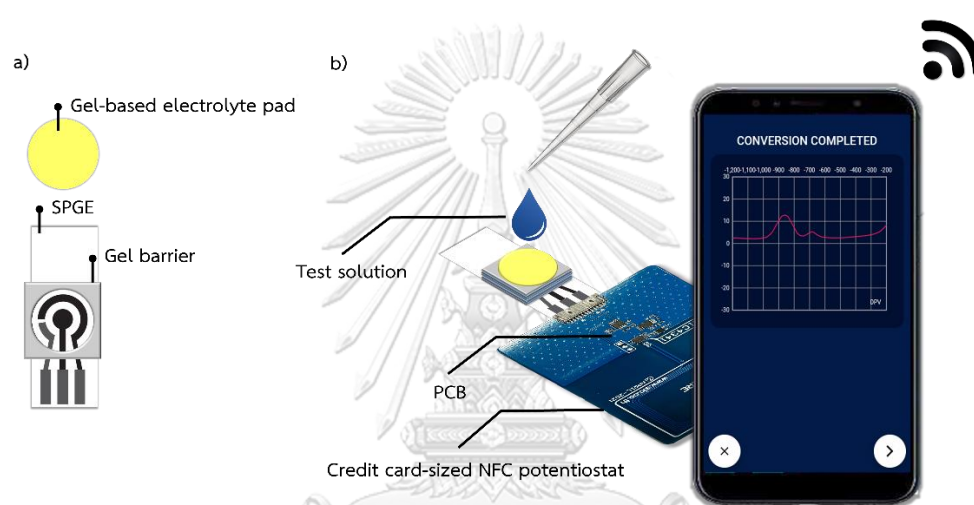


**Figure 11** Scheme of the gel-based electrolyte platform and its operation

### 3.3.5 Real sample analysis

For real sample analysis application, the performance of the developed pectin gel-based electrolyte device was examined using five cannabis-infused drinking water samples. The commercial cannabis-infused drinking water samples were purchased from a Thai supermarket. Based on the first observations (preliminary), it appears that these drinks did not contain any Cd(II) or Pb(II). Consequently, a standard solution containing Cd(II) and Pb(II) was spiked into the tested solutions to the appropriate concentrations in order to validate the method. After that, each tested solution was dropped straight onto the sample pad and the electrochemical measurement was performed. Using differential pulse anodic stripping voltammetry (DPASV), the

calibration curves of the two metals were used to calculate their concentrations. The recovery of each metal was used to evaluate the accuracy of the proposed sensor and compared with those obtained from an inductively coupled plasma-optical emission spectrometer (ICP-OES, iCAP 6500 series, Thermo Scientific, USA). The operating parameters as presented in Table 3 were utilized to execute the ICP-OES analysis.

**Table 3** The operating parameters of ICP-OES.

ICP Spectrometer	Thermo Scientific iCAP 6500
RF Generator	27.12 MHz
RF Power	1150 W
Plasma Gas Flow	12.0 L/min
Auxiliary Gas Flow	0.50 L/min
Nebulizer Gas Flow	0.60 L/min
Sample Uptake	0.90 mL/min
Nebulizer	Concentric
Spray Chamber	Cyclonic
Plasma Viewing	Axial
Wavelengths	As 189.042 nm Cd 228.802 nm Cr 283.563 nm Hg 184.950 nm Pb 220.353 nm

## CHAPTER IV

### RESULTS AND DISCUSSION

The results for the characterization of the gel-based electrolyte platform and discussion of the optimized experimental conditions are covered in this chapter. Additionally, descriptions are provided for the analytical performance, interference investigation, stability study, and real sample analysis.

#### 4.1 Surface morphology of pectin gel-based electrolyte

The surface morphologies of a plain filter paper and those containing the gel-based electrolyte were observed using scanning electron microscopy (SEM) and energy-dispersive X-ray fluorescence (EDXRF) techniques. The surface of the bare filter paper in Fig. 12A is slightly rough with cellulose flake due to its nature, while the surface of the biopolymeric gel-based electrolyte covered on filter paper in Fig. 12B is smoother. Furthermore, the pectin electrolyte is shown in Fig. 12C as a thin film that covers the cellulose structure of filter paper and has tiny globular particles widely scattered across its surface. Nearly equal atomic percentages of K and Cl were found by the elemental analysis of these particles using the EDXRF technique (Fig. 13), indicating a successful integration of the supporting electrolyte into the gel material.

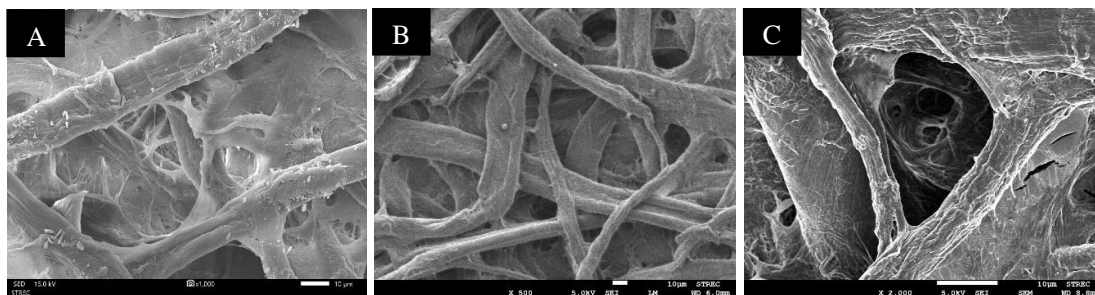


**Figure 12** SEM images of a bare filter paper (A), and biopolymeric gel-based electrolyte covered filter paper (B-C).

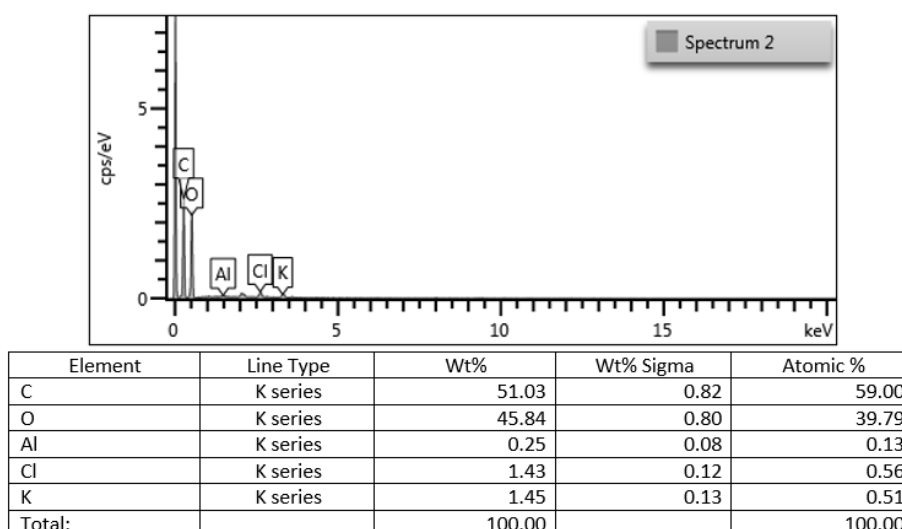


**Figure 13** Elemental analysis of the gel-based electrolyte pad by energy dispersive X-ray fluorescence (EDXRF).

#### 4.2 Electrochemical characterization of modified electrodes for Cd(II) and Pb(II) determination

The development of novel electrochemical sensors has resulted in a great deal of the electrochemical modification process with metallic nanoparticles. Of these, bismuth nanomaterials are well known for being biological substrate and environmentally friendly. In a recent study, the electrochemical modification of screen-printed carbon electrode (SPCE) with bismuth nanoparticles proved to be an effective method for creating a device (BiNPs/SPCE) for measuring heavy metal ions in



real sea water samples (44). In addition, the BiNPs' great surface catalytic activity, large surface-to-volume ratio, high conductivity, and adsorptive capacity make them an extremely promising electrode modification for electrochemical sensing applications (45). As a result, a number of electrodes were first examined for their analytical performance with regard to the simultaneous electrochemical detection of Cd(II) and Pb(II) using a conventional liquid electrolyte. These electrodes consisted of a conventional screen-printed graphene electrode (SPGE), Bi in situ electrode (Bi/SPGE), BiNP electrode (BiNP/SPGE), and Bi in situ with BiNP electrode (Bi/BiNP/SPGE). Fig. 14 shows the DPASV results of  $0.5 \mu\text{g mL}^{-1}$  Cd(II) and  $0.5 \mu\text{g mL}^{-1}$  Pb(II) in 0.1 M HCl obtained from using the traditional SPGE and several of the previously stated modified SPGEs. The oxidation peak of Pb(II) was hardly discernible at the potential of -0.6 V vs. Ag/AgCl (b), while the oxidation peak of Cd(II) was undetectable with the unmodified SPGE. On the other hand, two distinct oxidation peaks of Cd(II) and Pb(II) at about -0.9 V and -0.6 V, respectively, were formed by the SPGE with Bi in situ (Bi/SPGE) on the electrode during the deposition process (c). The two unique peaks with increased sensitivity are readily explained by the alloy species which accumulate on the electrode surface between Bi and the metal analytes, facilitating their oxidation and raising their anodic stripping current. Furthermore, at the Bi film's surface, Bi(III) can be converted to Bi(0) to create a Bi film electrode (BiFE). The total detection performance of this device can be significantly enhanced since the Bi film has a higher electroactive surface, which boosts both mass transfer and electron transfer rates (46). A similar outcome was obtained when BiNPs were modified to the SPGE but with a slightly reduced sensitivity (d). The screen-printed graphene electrode (Bi/BiNP/SPGE) modified with both Bi in situ and BiNPs modification yielded the highest overall performance in terms of peak separation and improved sensitivity (e).

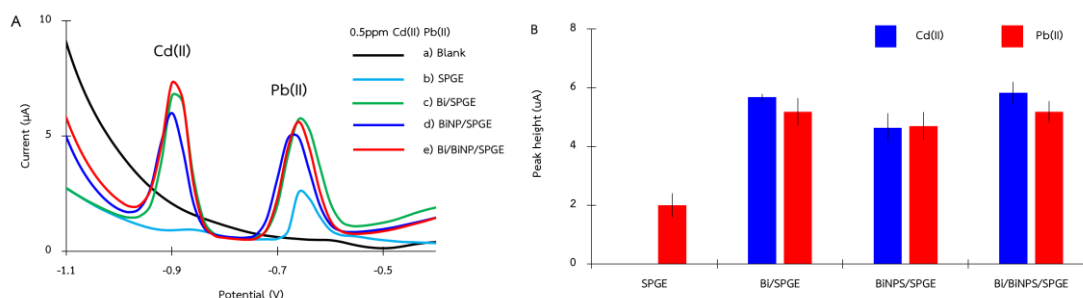


**Figure 14** DPV curves (A) and anodic currents (B) of blank solution (0.1 M HCl) and 0.5  $\mu\text{g mL}^{-1}$  Cd(II) and Pb(II) in 0.1 M HCl (liquid electrolyte platform).

However, the liquid electrolyte also has a significant impact on how well these electrodes operate for on-site analysis. It is not very convenient to carry around for on-site applications because these liquid electrolytes need to be carefully prepared by skilled users in order to get the best results. The gel-based electrolyte created in this work was suggested as a substitute and as an electrochemical platform that is ready for use. It has the advantages of being lightweight, easier to handle, more stable, and having a structural design that can be adjusted without leaking electrolyte.

Initially, the acetate buffer-pectin gel electrolyte platform and the Bi/BiNP/SPGE were used for the electrochemical characterization of Cd(II) and Pb(II). For the purpose of Cd(II) and Pb(II) detection, pectin was pre-mixed with acetate buffer electrolyte in this preliminary investigation before casting in order to increase its ability to resist pH variations during dissolution (47). Similar to those produced by an ordinary liquid electrolyte, Figure 15 displays well-defined current peaks of Cd(II) and Pb(II) (b) achieved by utilizing the Bi/BiNP/SPGE with gel-based electrolyte. However, the peak currents of both Pb(II) and Cd(II) were considerably lower than those of the liquid electrolyte system. This is likely because the carboxylic groups of the pectin biopolymeric network adsorb these metal ions (48). Pb(II) had a more severe depletion than Cd(II) mainly driven by its higher binding affinity towards pectin. An additional electrode alteration was implemented in an effort to address this issue. Recently, Au

and Bi nanoparticles (NPs) modified electrodes have been receiving substantial attention previously in the detection of heavy metal ions because of their outstanding electrocatalytic activity, ease of manufacture, and low toxicity (41). Therefore, a modified gel-based electrolyte was introduced with bimetallic Au-Bi. Once compared to monometallic catalyst (b), the peak currents of Cd(II) and Pb(II) were higher when Au-Bi modification was used (c). This can be attributed to the bimetallic system's electrochemical catalytic activity, which allows them to alloy with Cd(II) and Pb(II) on the electrode surface and facilitate electron transport during the detection process, resulting in the signal increase. For another bimetallic enhancement, antimony (Sb) has apparently been utilized to fabricate antimony-based film electrodes (SbFE) to improve electrode performance, antimony was chosen as an additional modifying agent on the SPGE (49). Using the bimetallic modifier (Sb-Bi) produced the highest peak currents of the two analytes (d) probably because the selectivity of Sb(III) towards Cd(II) and Pb(II) ions was higher than Au(III). Additionally, Rhodamine B (RhB) as a modified material only displayed a Cd(II) signal because RhB is a cationic dye that can turbulently transport cationic heavy metals (50) (e). Meanwhile, the electrochemical signals of Cd(II) and Pb(II) using EDTA (f) were absent apparently because EDTA can form highly stable chelates with pectin and metal ions. Pectin-EDTA-Pb(II), a large molecule (51), moves slowly to the electrode surface. As a result, Cd(II) and Pb(II) signals were absent. Overall, it appears that the addition of the Sb-Bi bimetallic catalyst enhanced the detection by increasing the peak current, thereby improving the sensitivity of the electrochemical measurement for Cd(II) and Pb(II) ions. As a result, the gel-based electrolyte platform was chosen to incorporate the bimetallic Sb-Bi modifier and investigated further.

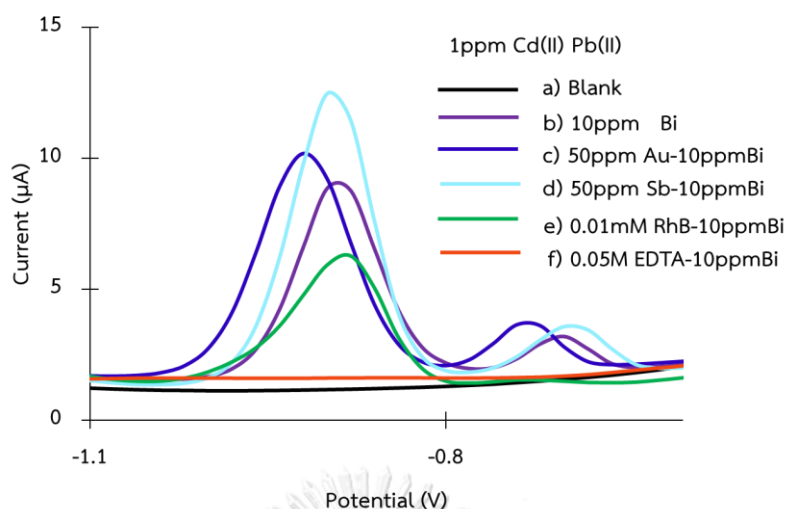


**Figure 15** DPV of blank solution and 1 ppm Cd(II) and Pb(II) containing modified gel-based electrolyte on Bi/BiNP/SPGE.

### 4.3 Optimization

#### 4.3.1 Device

Considering that the concentration gradient's mass transfer may be influenced by distance, the gap thickness may therefore have a major effect on the buildup of Cd(II) and Pb(II) on the sensor's surface. In the range of 300 to 1300  $\mu\text{m}$ , different gap thicknesses between the electrode and the gel-based electrolyte pad were used to study the DPV stripping current of the target analytes. An increase in the distance usually results in a stronger signal current because a larger vertical flow can facilitate analyte's mass transfer more effectively. Excessive spacing, however, unnecessarily lengthens the analyte's path to the electrode surface and could have unfavorable effects. As seen in Fig. 16, the optimal current responses of both target analytes were established using a gap thickness of 800  $\mu\text{m}$ .

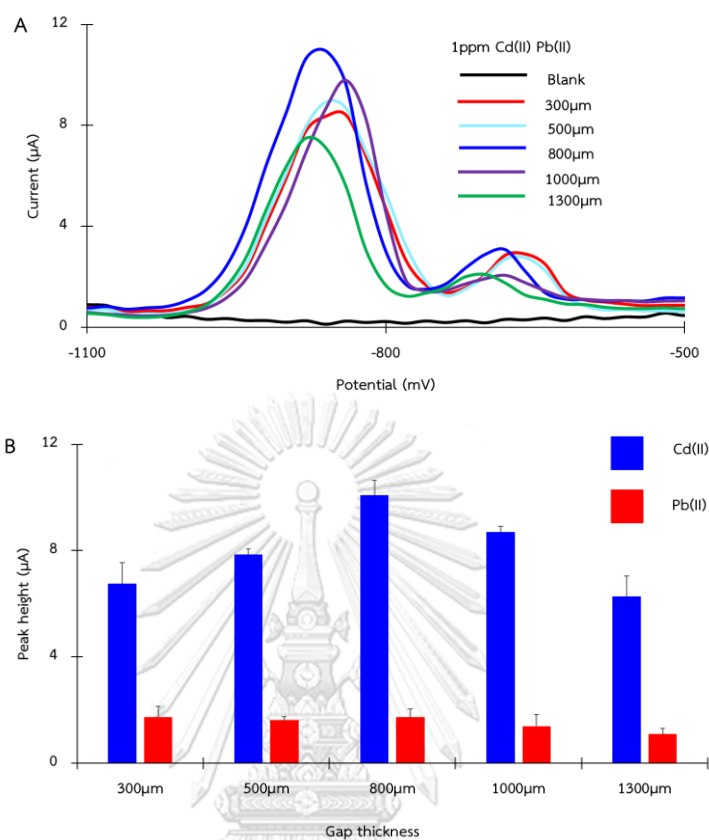


**Figure 16** Effect of optimized experimental parameters for the determination of Cd(II) and Pb(II) such as DPV curve (A) and anodic currents (B) of gap thickness of the device.

#### 4.3.2 Composition of gel-based electrolyte

The formation of a gel-based electrolyte is mostly dependent on the kind of biopolymer that is utilized, and more significantly, on its physical and chemical characteristics. Viscosity is one of these characteristics that influences the target analyte's mass transfer during the electrochemical determination stage. As a result, the researchers' goal was to investigate how various biopolymer types affect the gel-based electrolyte system's ability to generate a gel for heavy metal detection. Several biopolymers, such as carboxymethyl cellulose (CMC), hydroxypropyl methylcellulose (HPMC), hydroxyethyl cellulose (HEC), pectin, and pullulan, were utilized to create gel-

based electrolytes and subsequently assessed. The biopolymeric CMC gel-based electrolyte (b) shows the lowest current caused by its high viscosity nature (52), as illustrated in Fig. 17. HEC and HPMC (c–d) demonstrated somewhat better but still inadequate current signals for the target analytes due to their swelling feature (53, 54). These polymers have a tendency to expand when they absorb water, which increases the distance between the electrode and the sample zone and reduces the mass transit of Pb(II) and Cd(II) ions to the electrode. Pectin-based electrolyte (e), on the other hand, was chosen as a model gel electrolyte for further investigation because it was able to produce distinct, well-defined, and sharply separated current peaks for both analytes with the highest signal to background among the biopolymers employed.

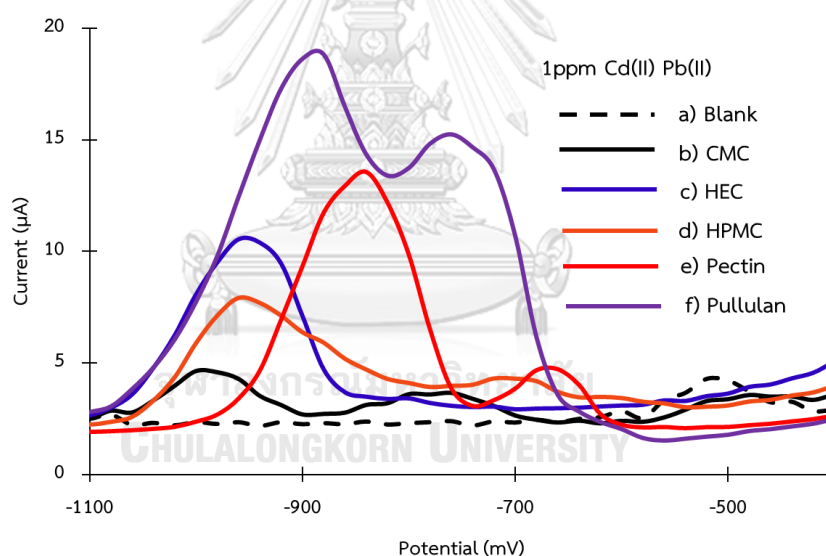


**Figure 17** Effect of biopolymers used as gel-based electrolyte for the determination of Cd(II) and Pb(II).

The impact of the pectin-based solution's pH was further investigated because this parameter can have a major influence on the buildup of Cd(II) and Pb(II) on the sensor surface (55) during the preconcentration phase of the electrochemical analysis. The investigation was carried out using DPV analysis to measure  $1 \mu\text{g mL}^{-1}$  Cd(II) and Pb(II)

in pectin solutions with pH values ranging from 2 to 12. The maximum stripping peak currents of both analytes were shown under extremely acidic conditions, i.e. pH 3, as illustrated in Fig. 18. Evidently, as a result of the hydrolysis of Bi(III) and precipitation of Bi(OH)<sub>3</sub> in the basic solution, the currents gradually decreased when the pH was raised (56).

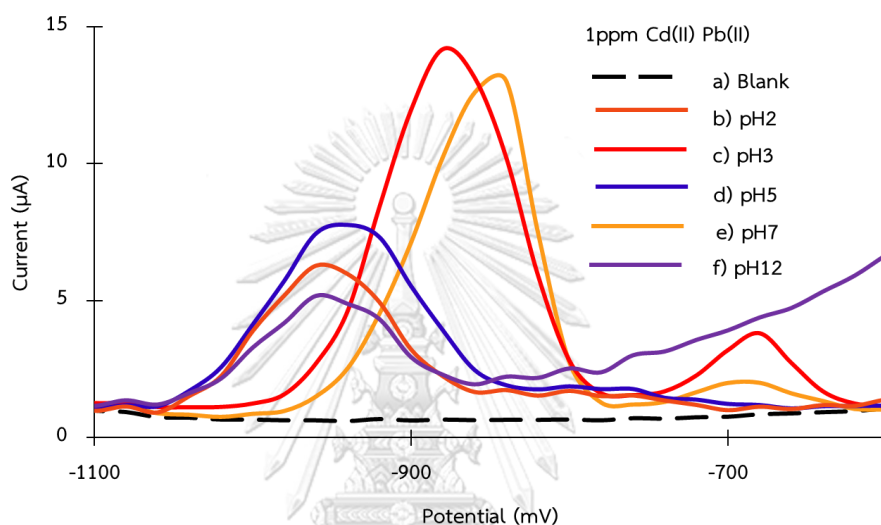


**Figure 18** Effect of various pH of gel-based electrolyte for the determination of Cd(II) and Pb(II).

The supporting electrolyte is one of the key components that influences the quality of an electrochemical measurement. For this reason, several electrolyte types, including potassium chloride, nitric acid, acetate buffer (pH 3), citric buffer (pH 3), and hydrochloric acid, were reviewed for how well they performed on the gel-based platform. Acidic electrolytes are frequently employed in anodic stripping voltammetry (ASV) as a supporting electrolyte to increase metal ion determination's sensitivity and selectivity (57). Both HCl and HNO<sub>3</sub> generated almost identical voltammograms with comparable peak currents for both analytes (e–f), as shown in Fig. 19. The oxidation peaks obtained with HNO<sub>3</sub>, however, showed a minor shift toward a more negative

potential. Since  $\text{HNO}_3$  is an oxidizing acid, it would thus be easier for both metals to oxidize, which would result in this transposition. Despite this, the presence of  $\text{Pb(II)}$  was not evidently addressed by either of the acidic electrolytes, as its currents were barely discernible. Using acetate buffer (pH 3) resulted in a voltammogram that was comparable to the previous two electrolytes but had better  $\text{Pb(II)}$  peak current (b). This improvement may be attributed to the more effective pH regulation of the buffer electrolyte. The sensitivity boost was also seen when citric buffer (pH3) was utilized (c), unfortunately, the oxidation peaks of both analytes were significantly widened and overlapped which may have been caused by the steric hindrance effect of this electrolyte. In the end, it was discovered that using  $\text{KCl}$  as a supporting electrolyte produced the best DPASV responses with sharply defined and strong current oxidation peaks (d).

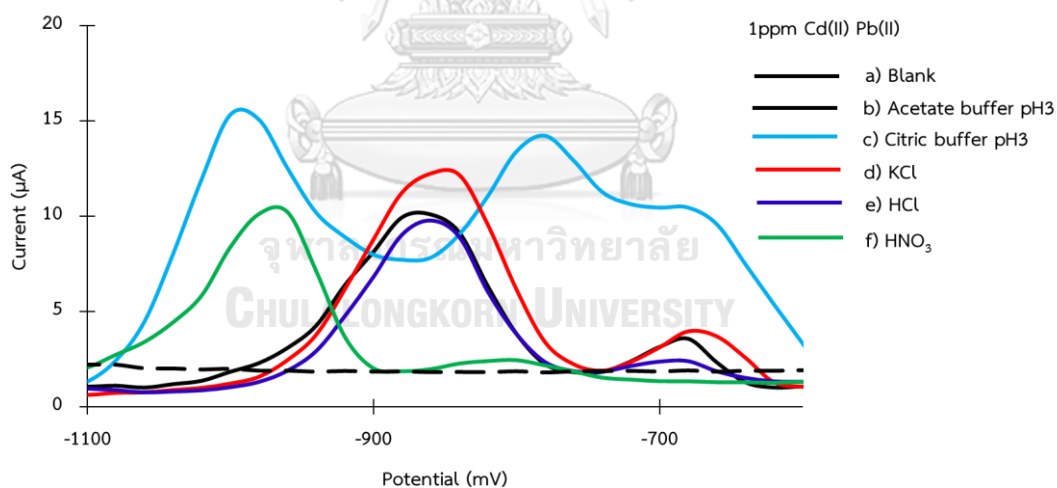


**Figure 19** Effect of optimized type of supporting electrolyte for the determination of  $\text{Cd(II)}$  and  $\text{Pb(II)}$ .

Since it can provide these beneficial qualities and be easily consolidated into the gel-based platform, the effect of  $\text{KCl}$  supporting electrolyte's concentration was next



investigated, and the outcome is shown in Fig. 20, Peak Cd(II) currents obtained with KCl in the 0.01-0.25 M range were similar, but there was a noticeable difference on the Pb(II) end, where the signal decreased with increasing KCl concentrations. The best electrochemical signals for both Cd(II) and Pb(II) was achieved with 0.025 M KCl and this was used for the duration of the investigation.

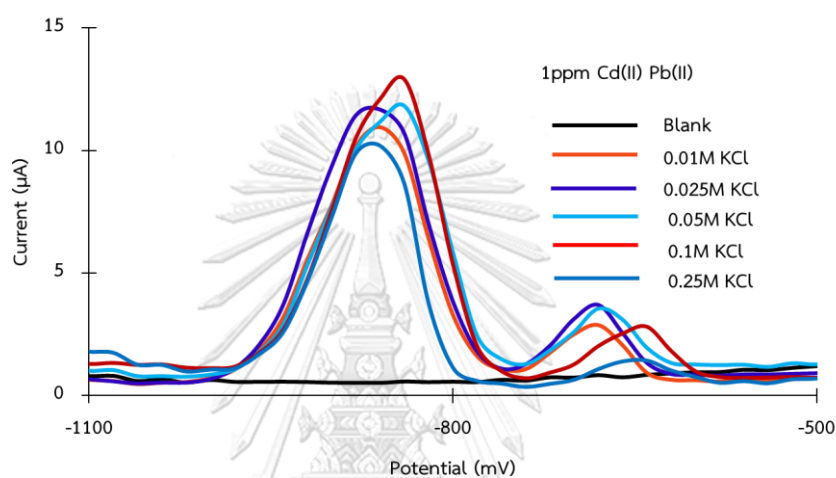


**Figure 20** Effect of optimized various concentration of supporting electrolyte for the determination of Cd(II) and Pb(II).

In addition, the gel formation and its dissolving behavior, which can affect the ion migration and its detection efficiency, are also major factors in determining the electrochemical performance of a gel electrolyte, apart from the supporting electrolyte. As a result, the impact of pectin concentration, an essential component of the gel-forming substance, was examined within the range of 1% w/v to 3% w/v. Figure 21. showed that the stripping current increased up to 1.5% pectin concentration before progressively declining after that. It was evident that a film electrolyte with a lower thickness and likely insufficient electrolyte storage capacity was produced by the reduced pectin concentration (e.g., 1%). Higher polymeric content, on the other hand, typically results in unduly thick films that are less able to absorb water, which

in turn causes inefficient breakdown and insufficient release of the supporting electrolyte (58). Using 1.5% pectin resulted in the best-performing gel electrolyte with the ideal film thickness and viscosity, as well as quick dissolving and electrolyte-releasing qualities.

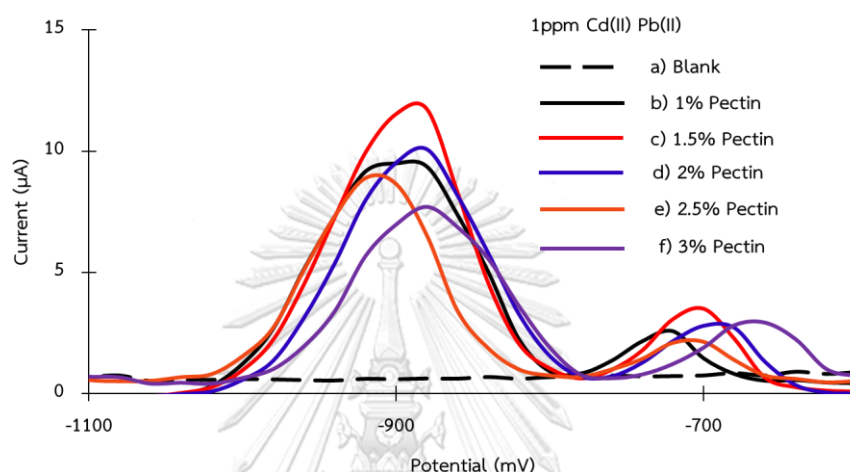


**Figure 21** Effect of pectin content for the determination of Cd(II) and Pb(II).

Furthermore, the Sb-Bi bimetallic alloy modified on the pectin-based electrolyte was used to enhance the anodic stripping voltammetry (ASV) on electrochemical detection of Cd(II) and Pb(II). It is well known that this bimetallic system raises the electrochemical signals of both analytes by improving the conductivity, stability, and catalytic activity of the electrode/electrolyte interface (59). Sb/Bi ratios in the range of 9:1, 7:3, 5:5, 3:7, and 1:9 were investigated in this study. The voltammograms produced by ASV analysis at -1.2 V for the pectin-based electrolyte solutions with specified concentration ratios of Sb(III) and Bi(III) ( $50 \mu\text{g mL}^{-1}$  total concentration) and  $1 \mu\text{g mL}^{-1}$  for each of Cd(II) and Pb(II) are shown in Fig. 22. When Sb was present in higher proportions, an increasing trend in the Cd(II) current signal was seen, likely because antimony has a better affinity to form an alloy with cadmium than with bismuth. In contrast, Pb(II) peak currents are much smaller, with the maximum peak current being

achieved with an equal quantity of Sb and Bi. Given that Pb is the less sensitive analyte, which is our primary concern, this ratio (0.5Sb0.5Bi) was selected as the ideal setting for more tests.

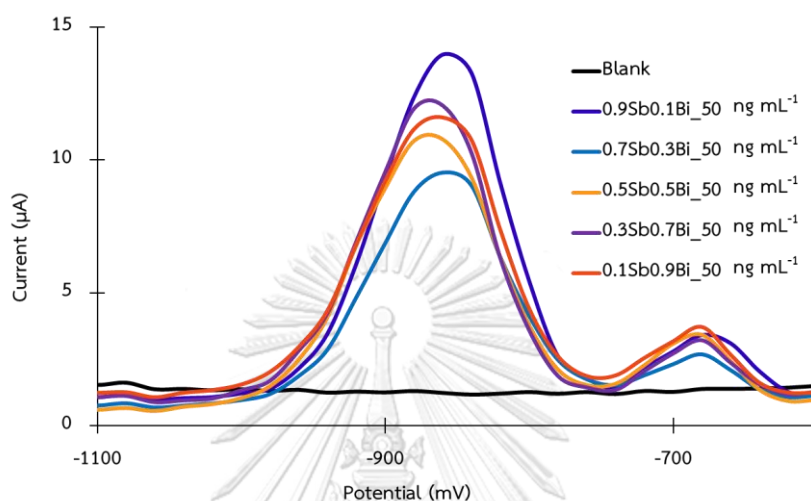


**Figure 22** Effect of the Sb/Bi concentration ratio for the determination of Cd(II) and Pb(II).

### 3.3.3 Electrode modification

Bismuth nanoparticles were added to the screen-printed graphene electrode utilized in this study for further improvement of its electrochemical activity and analyte detectability. To fabricate BiNP/SPGE, several concentrations of BiNPs (0.25-2%) were added into graphene ink as a pre-mixed formulation and assessed. Different loading of BiNPs had no effect on the peak morphologies of either analyte, as seen in Fig. 23, but they did have an impact on their peak currents. The current had an early tendency to grow and then began to decrease as the BiNPs increased. This behavior may have been caused by oversaturation of the BiNPs, which negatively impacted the conductivity of the graphene-based electrode. Because Pb(II) has a greater affinity towards Bi than the other analyte, less BiNPs (0.5%) was required to obtain the maximal peak current. The optimization focused mainly on enhancing the Pb signal because the Cd(II) sensitivity

was already high enough for NFC detection, as a result, 0.5%BiNP was selected as the ideal modifier concentration.

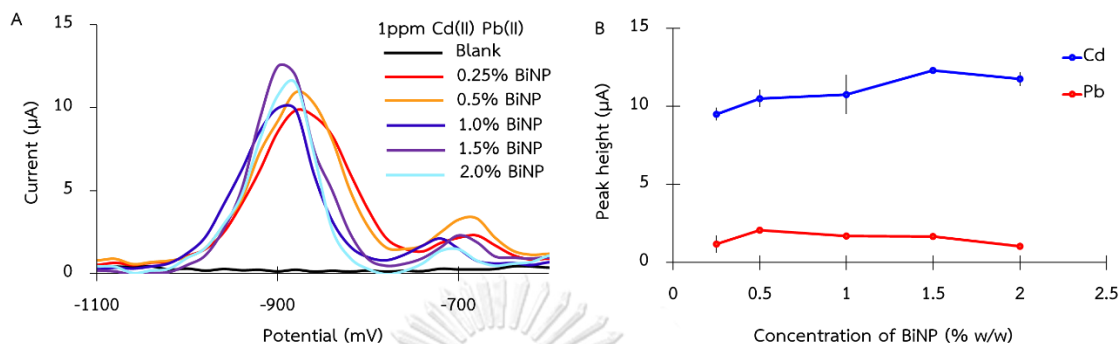


**Figure 23** Effect of concentration of BiNP for the determination of Cd(II) and Pb(II).

### 3.3.4 Electrochemical parameters

The important electrochemical measurement operating parameters including the deposition potential, deposition time, potential amplitude, and scan rate were next examined after putting all of the earlier configurations into practice. The impacts of these factors on the peak currents of Pb(II) and Cd(II) as well as the voltammograms are shown in Figs. 24. The optimal outcome was definitively shown to be achieved at a deposition potential of -1.2 V, a deposition period of 300 s, a potential amplitude of 100 mV, and a scan rate of 100 mV/s.

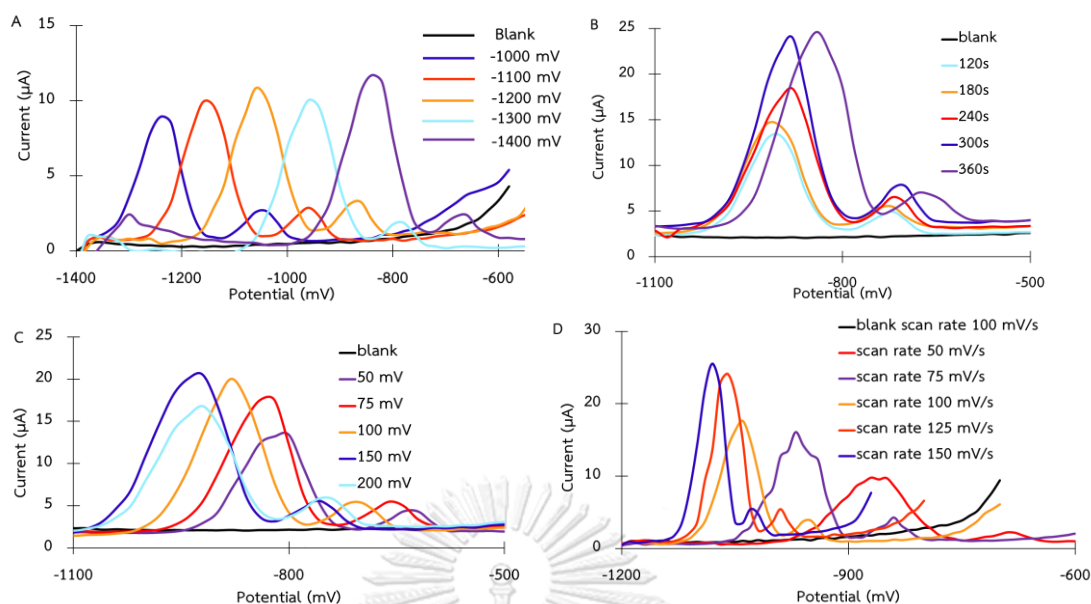


**Figure 24** Effect of deposition potential (A), deposition time (B), amplitude (C) and step potential (D) to the stripping current of  $1000 \text{ ng mL}^{-1}$  Cd(II) and Pb(II); the signals are shown as means of the measured values ( $n=3$ ).

### 3.4 Analytical performance of the biopolymeric gel-based electrolyte platform

For the simultaneous measurement of Cd(II) and Pb(II) by DPASV, the electrochemical performance of the created gel-based electrolyte was assessed using a near field communication (NFC) potentiostat connected with a smartphone. Excellent linearities were established with a good correlation coefficient ( $R^2$ ) of 0.987 for Cd(II) and 0.962 for Pb(II), respectively. As illustrated in Fig. 25, well defined peak responses were obtained for both analytes in the range of  $150$  to  $1500 \text{ ng mL}^{-1}$  for cadmium and  $200$ - $1500 \text{ ng mL}^{-1}$  for lead. For Cd(II) and Pb(II), the estimated limit of detection (ascertained by  $3S/N$ ) were  $50.98 \text{ ng mL}^{-1}$  and  $40.80 \text{ ng mL}^{-1}$ , respectively.

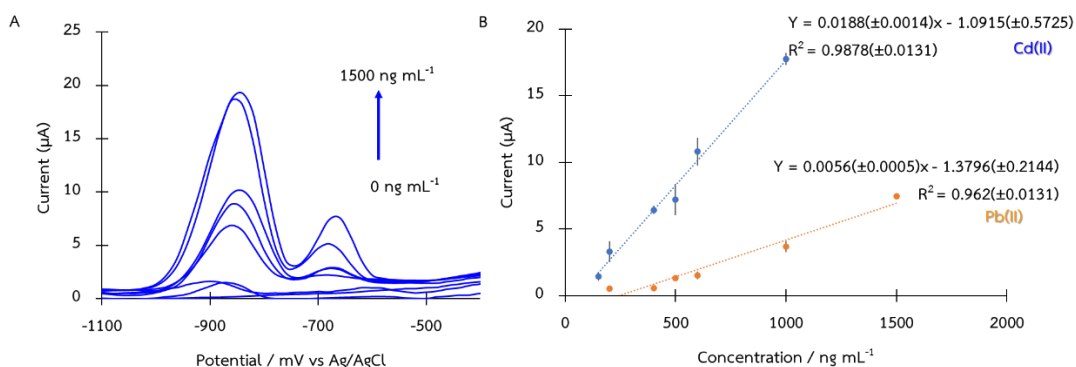


**Figure 25** (A) DPVs of blank solution (milli-Q water), Cd(II), and Pb(II) at concentrations of 0-1500 ng mL<sup>-1</sup> using gel-based electrolyte on a Sb-Bi modified screen-printed electrode. (B) A linear relationship between the oxidative currents and concentrations of Cd(II) and Pb(II).

As illustrated in Fig. 26, the repeatability, given as relative standard deviation (RSD), of the suggested device was less than 10.4% (n=10) for the determination of Cd(II) and Pb(II) at 400, 600, and 1000 ng mL<sup>-1</sup>. Additionally, the constructed platform's stability was evaluated over a prolonged length of time. When the device was stored for more than three weeks at room temperature in a dry state, there was no discernible change of more than  $\pm 10\%$  of the current signal for 1000 ng mL<sup>-1</sup> Cd(II) and Pb(II), as shown in Fig. 27.

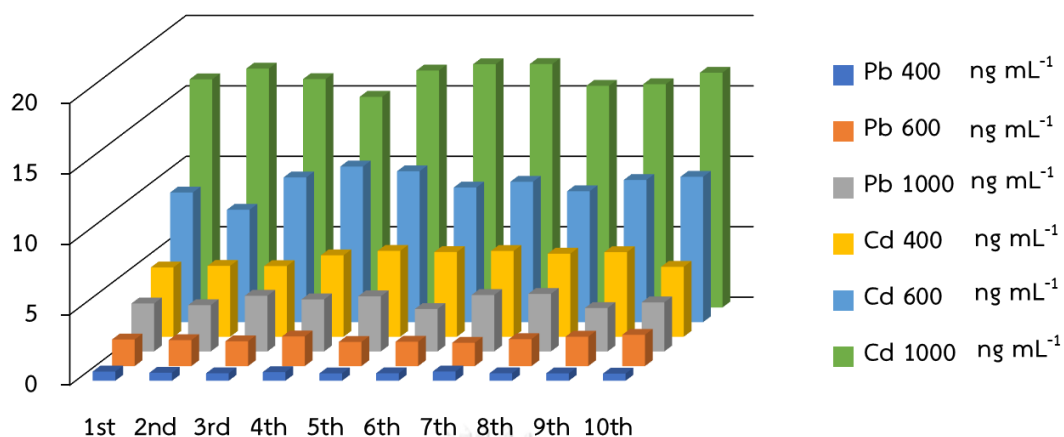


**Figure 26** The reproducibility of the Sb-Bi/BiNP/SPGE using pectin-based electrolyte for the determination of 400-1000 ng mL<sup>-1</sup> Cd(II) and Pb(II); the signals are shown as peak height of the measured values (n=10).

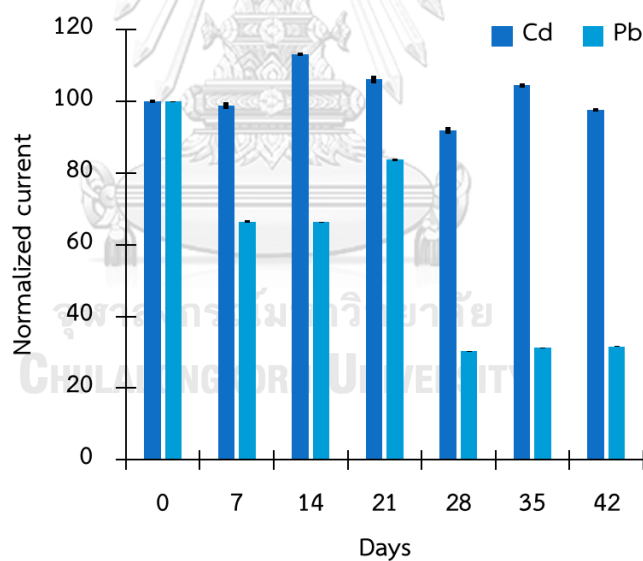


**Figure 27** Long-term stability of Sb-Bi/BiNP/SPGE using pectin-based electrolyte; Cd(II) 1000 ng mL<sup>-1</sup> and Pb(II) 1000 ng mL<sup>-1</sup>; the signals are shown as means of the measured values (n=3).

The combination of the developed pectin-based gel electrolyte, modified screen-printed graphene electrode, and NFC potentiostat was able to perform the

electrochemical determination of both Cd(II) and Pb(II) to an extremely good level, as these analytical figures of merit clearly validated. Table 4 compares the analytical performance of the suggested platform with a few other electrochemical sensors that have been previously published in recent years and whose electrodes have been similarly modified by a variety of composite materials, such as bismuth ion, antimony ion, or biopolymers. In addition to having an excellent detection limit and a broad linear dynamic range for the simultaneous measurement of Pb(II) and Cd(II), our sensing platform is inexpensive to construct and made of environmentally safe materials. Although the present platform's LOD and linear range might not be as good as some of the prior studies, the incredible simplicity of our device easily makes up for this shortcoming, especially when used for on-site analysis.

**Table 4** Comparison of the analytical performance of the Sb-Bi/BiNP/SPGE using pectin-based electrolyte with other works for heavy metals determination using electrochemical sensors.

Materials	Methods	Heavy metals detected	Linear Range (ng mL <sup>-1</sup> )	LOD (ng mL <sup>-1</sup> )	Ref.
GCE/MWCNTs-PEC <sup>a</sup>	SWASV <sup>b</sup>	Cu	6.35x10 <sup>5</sup> - 6.35x10 <sup>7</sup>	5.72x10 <sup>5</sup>	(60)
Bi/CMC-GCE <sup>c</sup>	DPASV	Cd	1.12x10 <sup>2</sup> - 1.12x10 <sup>5</sup>	84.31	(13)
Bi-C SPE <sup>d</sup>	SWASV	Cd, Pb	1-50	1.5, 2.3	(61)
Bi-SbFES <sup>e</sup>	SWASV	Zn, Cd, Pb	3.0–29.1, 1.0–65.4, 1.0–119.3	0.5, 0.5, 0.7	(42)



Materials	Methods	Heavy metals detected	Linear Range (ng mL <sup>-1</sup> )	LOD (ng mL <sup>-1</sup> )	Ref.
Sb-Bi/BiNP/SPGE using pectin-based electrolyte	DPASV	Cd,Pb	1.5x10 <sup>2</sup> - 1.0x10 <sup>3</sup> 2.0x10 <sup>2</sup> - 1.5x10 <sup>3</sup>	50.98, 40.80	This work

<sup>a</sup> Glassy carbon electrode modified with multi-walled carbon nanotubes and pectin;

<sup>b</sup> SWASV: square wave anodic stripping voltammetry; <sup>c</sup> Bismuth and carboxymethyl cellulose modified glassy carbon electrode; <sup>d</sup> Bismuth nanoparticle porous carbon nanocomposite screen-printed electrode; <sup>e</sup> Bismuth-antimony film glassy carbon electrodes.

### 3.5 Interference study

The selectivity and possible interferences of the proposed device was next investigated. Several common ions, which might be present in the practical samples, such as Fe(II), Fe(III), Zn(II), Al(III), Mg(II), Cu(II), Ni(II), Ca(II), Na(I), and Mn(II), were added at a 1-fold mass ratio on top of the analyte ions at a concentration of 1 µg mL<sup>-1</sup>. As shown in Fig. 28, it was found that almost all of the investigated ions, aside from Cu(II) and Ni(II), had no detrimental effects on the current signal of either Cd(II) or Pb(II). However, the presence of Cu(II) and Ni(II) at a 1-fold mass ratio decreased the oxidation current of Cd by around 10%. Thus, it can be said that the created microfluidic electrochemical device is essentially devoid of most interferences and quite selective.

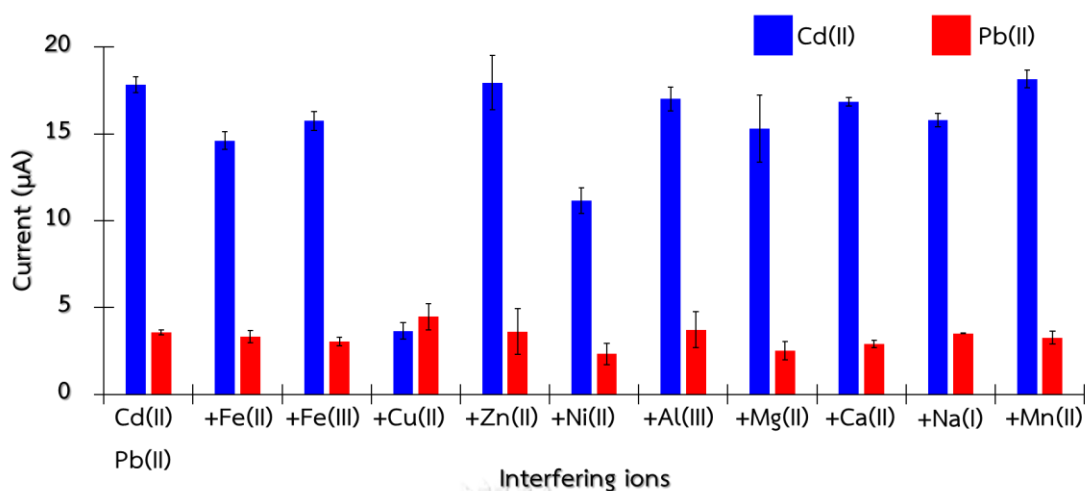


**Figure 28** Influence of common ions on the current signal of Cd(II) (a) and Pb(II) (b), ratios are given as  $m(\text{interferent}):m(\text{Cd(II)/Pb(II)})$ ; the signals are shown as means of the measured values ( $n=3$ ).

### 3.6 Application in real sample

The recently created pectin-based electrolyte platform was used as a device that was ready to use for measuring Pb(II) and Cd(II) in actual samples. Because cannabis is known to be a plant commonly contaminated with heavy metals from soil, water, or the air, it was selected as the subject of analysis. Five cannabis-infused drinking water samples were collected from nearby retailers and subjected to direct analysis for lead and mercury (Pb and Cd) under the optimal operating conditions. No sample pretreatment was performed. These samples had not previously been contaminated with Cd or Pb, thus they were spiked with standards ( $600$  and  $1000 \text{ ng mL}^{-1}$ ), and their recovery percentage served as technique validation. Together with the comparative data from the conventional ICP-OES method, the results were displayed in Table 5-6. It was discovered that the percentage recoveries of Pb(II) and Cd(II) were from 80-110% and 87-110%, respectively. There was no significant difference between the two approaches using a t-test with a 95% confidence level. Therefore, it is technically possible to conclude that the created platform may be employed with high accuracy,

dependability, and ultimate convenience to determine Pb(II) and Cd(II) in cannabis drinking water samples.

**Table 5** Recovery tests of the proposed sensor and conventional method for the simultaneous determination of Cd(II) in cannabis-infused drinking water samples (n = 3).

Cannabis drinking water samples	Spiked ng mL <sup>-1</sup>	Cd							
		Proposed sensor				ICP-OES			
		Found				Found			
		$\bar{x}$	$\pm$	SD	%recovery	$\bar{x}$	$\pm$	SD	%recovery
ng mL <sup>-1</sup>				ng mL <sup>-1</sup>					
A	non-spike	ND				-			
	600	661	$\pm$	2	110	616	$\pm$	0	103
	1000	1089	$\pm$	6	109	1040	$\pm$	0	104
B	non-spike	ND				-			
	600	653	$\pm$	15	109	580	$\pm$	1	97
	1000	936	$\pm$	43	94	982	$\pm$	1	98
C	non-spike	ND				-			
	600	664	$\pm$	4	110	597	$\pm$	1	100
	1000	922	$\pm$	25	92	995	$\pm$	2	100
D	non-spike	ND				-			
	600	655	$\pm$	24	109	614	$\pm$	1	102
	1000	1098	$\pm$	13	110	1006	$\pm$	1	101
E	non-spike	ND				-			
	600	524	$\pm$	36	87	678	$\pm$	1	110
	1000	944	$\pm$	24	94	1083	$\pm$	2	108

\*ND is non-detected

**Table 6** Recovery tests of the proposed sensor and conventional method for the simultaneous determination of Pb(II) in cannabis-infused drinking water samples (n = 3).

Cannabis drinking water samples	Pb								
	Spiked ng mL <sup>-1</sup>	Proposed sensor				ICP-OES			
		Found			%recovery	Found			%recovery
		$\bar{x}$	$\pm$	SD		$\bar{x}$	$\pm$	SD	
		ng mL <sup>-1</sup>				ng mL <sup>-1</sup>			
A	non-spike	ND			-	ND			-
	600	534	$\pm$	26	89	585	$\pm$	1	97
	1000	803	$\pm$	49	80	988	$\pm$	3	99
B	non-spike	ND			-	ND			-
	600	573	$\pm$	30	95	533	$\pm$	1	89
	1000	802	$\pm$	34	80	910	$\pm$	1	91
C	non-spike	ND			-	ND			-
	600	593	$\pm$	16	99	558	$\pm$	1	93
	1000	957	$\pm$	62	96	929	$\pm$	2	93
D	non-spike	ND			-	ND			-
	600	556	$\pm$	7	93	579	$\pm$	1	97
	1000	802	$\pm$	21	80	964	$\pm$	4	96
E	non-spike	ND			-	ND			-
	600	653	$\pm$	2	109	597	$\pm$	1	100
	1000	1100	$\pm$	63	110	967	$\pm$	3	97

\*ND is non-detected

## CHAPTER V

### CONCLUSIONS AND FUTURE PERSPECTIVE

#### 5.1 Conclusion

In this work, a new platform of biopolymeric gel-based electrolyte as a ready-to-use device for the simultaneous determination of Cd(II) and Pb(II) using Sb-Bi modified screen-printed electrode is presented. To demonstrate the portability and accessibility of the system, a smartphone-based electrochemical analysis was performed via near-field communication (NFC) potentiostat card coupled with the proposed device. A ready-to-use biopolymeric gel-based electrolyte sensor offers many advantages including ease of use, simple preparation, low-cost, portability, biodegradation, biocompatibility, and high stability. The developed platform was successfully applied for the simultaneous detection of Cd(II) and Pb(II) in cannabis drinking water samples with satisfactory results.

#### 5.2 Future perspective

In the future work, a development of this platform will achieve higher sensitivity and wide range application in other heavy metals.

## REFERENCES

1. Ding Q, Li C, Wang H, Xu C, Kuang H. Electrochemical detection of heavy metal ions in water. *Chem Commun (Camb)*. 2021;57(59):7215-31.
2. Rojas-Romo C, Aliaga ME, Arancibia V, Gomez M. Determination of Pb(II) and Cd(II) via anodic stripping voltammetry using an in-situ bismuth film electrode. Increasing the sensitivity of the method by the presence of Alizarin Red S. *Microchemical Journal*. 2020;159.
3. Craven CB, Wawryk N, Jiang P, Liu Z, Li XF. Pesticides and trace elements in cannabis: Analytical and environmental challenges and opportunities. *J Environ Sci (China)*. 2019;85:82-93.
4. Viviers HJ, Petzer A, Gordon R. An assessment of heavy metal contaminants related to cannabis-based products in the South African market. *Forensic Science International: Reports*. 2021;4.
5. Karimi-Maleh H, Karimi F, Alizadeh M, Sanati AL. Electrochemical Sensors, a Bright Future in the Fabrication of Portable Kits in Analytical Systems. *Chem Rec*. 2020;20(7):682-92.
6. Muthukrishnan M, Shanthi C, Selvasekarapandian S, Manjuladevi R, Perumal P, Chrishtopher Selvin P. Synthesis and characterization of pectin-based biopolymer electrolyte for electrochemical applications. *Ionics*. 2018;25(1):203-14.
7. Chen C, Niu X, Chai Y, Zhao H, Lan M, Zhu Y, et al. Determination of Lead(II) Using Screen-Printed Bismuth-Antimony Film Electrode. *Electroanalysis*. 2013;25(6):1446-52.
8. Andrade JR, Raphael E, Pawlicka A. Plasticized pectin-based gel electrolytes. *Electrochimica Acta*. 2009;54(26):6479-83.
9. Charoenkitamorn K, Chotsuwan C, Chaiyo S, Siangproh W, Chailapakul O. A new ready-to-use gel-based electrolyte for paraquat sensor. *Sensors and Actuators B: Chemical*. 2020;315.
10. Ledwon P, Andrade JR, Lapkowski M, Pawlicka A. Hydroxypropyl cellulose-based gel electrolyte for electrochromic devices. *Electrochimica Acta*. 2015;159:227-33.

11. Vahini M, Muthuvinayagam M. AC impedance studies on proton conducting biopolymer electrolytes based on pectin. *Materials Letters*. 2018;218:197-200.
12. Zambuzi GC, Camargos CHM, Ferreira MP, Rezende CA, de Freitas O, Francisco KR. Modulating the controlled release of hydroxychloroquine mobilized on pectin films through film-forming pH and incorporation of nanocellulose. *Carbohydrate Polymer Technologies and Applications*. 2021;2.
13. Primo CM, Buffon E, Stradiotto NR. A carbon nanotubes-pectin composite for electrochemical determination of copper in aviation biokerosene by anodic stripping voltammetry. *Fuel*. 2021;302.
14. Tchounwou PB, Yedjou CG, Patlolla AK, Sutton DJ. Heavy metal toxicity and the environment. *Exp Suppl*. 2012;101:133-64.
15. Zhai Q, Narbad A, Chen W. Dietary strategies for the treatment of cadmium and lead toxicity. *Nutrients*. 2015;7(1):552-71.
16. Purushotham D, Rashid M, Lone MA, Rao AN, Ahmed S, Nagaiah E, et al. Environmental impact assessment of air and heavy metal concentration in groundwater of Maheshwaram watershed, ranga reddy district, Andhra Pradesh. *Journal of the Geological Society of India*. 2013;81(3):385-96.
17. Mukherjee I, Singh UK, Singh RP, Anshumali, Kumari D, Jha PK, et al. Characterization of heavy metal pollution in an anthropogenically and geologically influenced semi-arid region of east India and assessment of ecological and human health risks. *Sci Total Environ*. 2020;705:135801.
18. Gupta S, Pandotra P, Gupta AP, Dhar JK, Sharma G, Ram G, et al. Volatile (As and Hg) and non-volatile (Pb and Cd) toxic heavy metals analysis in rhizome of *Zingiber officinale* collected from different locations of North Western Himalayas by Atomic Absorption Spectroscopy. *Food Chem Toxicol*. 2010;48(10):2966-71.
19. Ioannidou MD, Zachariadis GA, Anthemidis AN, Stratis JA. Direct determination of toxic trace metals in honey and sugars using inductively coupled plasma atomic emission spectrometry. *Talanta*. 2005;65(1):92-7.
20. Mohamed R, Zainudin BH, Yaakob AS. Method validation and determination of heavy metals in cocoa beans and cocoa products by microwave assisted digestion

technique with inductively coupled plasma mass spectrometry. *Food Chem.* 2020;303:125392.

21. <Allen\_J\_Bard\_Larry\_R\_Faulkner[1] electrochemistry.pdf>.

22. Oberacher H, Pitterl F, Erb R, Plattner S. Mass spectrometric methods for monitoring redox processes in electrochemical cells. *Mass Spectrom Rev.* 2015;34(1):64-92.

23. Dali M, Zinoubi K, Chrouda A, Abderrahmane S, Cherrad S, Jaffrezic-Renault N. A biosensor based on fungal soil biomass for electrochemical detection of lead (II) and cadmium (II) by differential pulse anodic stripping voltammetry. *Journal of Electroanalytical Chemistry.* 2018;813:9-19.

24. Manisankar P, Selvanathan G, Viswanathan S, Gurumallesh Prabu H. Electrochemical Determination of Some Organic Pollutants Using Wall-Jet Electrode. *Electroanalysis.* 2002;14(24):1722-7.

25. Ong CS, Ng QH, Low SC. Critical reviews of electro-reactivity of screen-printed nanocomposite electrode to safeguard the environment from trace metals. *Monatshefte für Chemie - Chemical Monthly.* 2021;152(7):705-23.

26. Dutta A, Nayak R, Selvakumar M, Devadiga D, Selvaraj P, Kumar SS. Graphite/copper nanoparticle-based high-performance micro supercapacitor with porous wet paper-based PVA-PVP blend polymer electrolyte. *Materials Letters.* 2021;295.

27. Cinti S, Talarico D, Palleschi G, Moscone D, Arduini F. Novel reagentless paper-based screen-printed electrochemical sensor to detect phosphate. *Anal Chim Acta.* 2016;919:78-84.

28. Cerdà V, Ferrer L, Avivar J, Cerdà A. Instrumentation. *Flow Analysis* 2014. p. 125-62.

29. Arce-Castro J, Vilasó-Cadre JE, Benítez-Fernández D, Rodríguez-de la Rosa H, Arada-Pérez MA. Effect of supporting electrolytes on voltammetry with manual staircase voltage scan. *The Journal of Engineering and Exact Sciences.* 2022;8(3):14235-01e.

30. Kreysa G, Ota K-i, Savinell RF. *Encyclopedia of Applied Electrochemistry* 2014.



31. Samsudin NA, Lim Y-C, Chang S-K, Heng I, Low FW, Shakeri M, et al. Titanium Dioxide Nanostructured Based Supercapacitors. *Encyclopedia of Energy Storage*2022. p. 361-73.
32. Sudhakar YN, Selvakumar M, Bhat DK. Biopolymer Electrolytes for Solar Cells and Electrochemical Cells. *Biopolymer Electrolytes*2018. p. 117-49.
33. Liao J, Chang F, Han X, Ge C, Lin S. Wireless water quality monitoring and spatial mapping with disposable whole-copper electrochemical sensors and a smartphone. *Sensors and Actuators B: Chemical*. 2020;306.
34. Kabalci E, Kabalci Y. Emerging wireless communication technologies for smart grid applications. *From Smart Grid to Internet of Energy*2019. p. 173-208.
35. Ye Y, Wu T, Jiang X, Cao J, Ling X, Mei Q, et al. Portable Smartphone-Based QDs for the Visual Onsite Monitoring of Fluoroquinolone Antibiotics in Actual Food and Environmental Samples. *ACS Appl Mater Interfaces*. 2020;12(12):14552-62.
36. Pungjunun K, Yakoh A, Chaiyo S, Siangproh W, Praphairaksit N, Chailapakul O. Smartphone-based electrochemical analysis integrated with NFC system for the voltammetric detection of heavy metals using a screen-printed graphene electrode. *Mikrochim Acta*. 2022;189(5):191.
37. Putro PA, Yudasari N, Maddu A. Spectroscopic Study on the Film of Polyvinyl Alcohol and Carboxymethyl Cellulose as Polymer Electrolyte Materials. *Journal of Physics: Conference Series*. 2020;1491(1).
38. Varshney PK, Gupta S. Natural polymer-based electrolytes for electrochemical devices: a review. *Ionics*. 2011;17(6):479-83.
39. Sun P, Xu K, Guang S, Xu H. Controlling assembly-induced single layer RGO to achieve highly sensitive electrochemical detection of Pb(II) via synergistic enhancement. *Microchemical Journal*. 2021;162.
40. Toghan A, Abd-Elsabour M, Abo-Bakr AM. A novel electrochemical sensor based on EDTA-NQS/GC for simultaneous determination of heavy metals. *Sensors and Actuators A: Physical*. 2021;322.
41. Wang W-J, Lu X-Y, Kong F-Y, Li H-Y, Wang Z-X, Wang W. A reduced graphene oxide supported Au-Bi bimetallic nanoparticles as an enhanced sensing platform for

simultaneous voltammetric determination of Pb (II) and Cd (II). *Microchemical Journal*. 2022;175.

42. Finšgar M, Petovar B. Novel in situ

Bi–Sb-Film Electrodes for Trace Heavy Metal Analysis. *Electroanalysis*. 2018;30(11):2781-92.

43. Zeinu KM, Hou H, Liu B, Yuan X, Huang L, Zhu X, et al. A novel hollow sphere bismuth oxide doped mesoporous carbon nanocomposite material derived from sustainable biomass for picomolar electrochemical detection of lead and cadmium. *Journal of Materials Chemistry A*. 2016;4(36):13967-79.

44. Cadevall M, Ros J, Merkoci A. Bismuth nanoparticles integration into heavy metal electrochemical stripping sensor. *Electrophoresis*. 2015;36(16):1872-9.

45. <21.pdf>.

46. Özyurt VH, Avcı O, Tepeli-Büyüksünetçi Y, Anık Ü. Bismuth film based electrochemical hydroxymethylfurfural sensor. *European Food Research and Technology*. 2023;249(6):1563-74.

47. Vasanthi Sridharan N, Mandal BK. Simultaneous Quantitation of Lead and Cadmium on an EDTA-Reduced Graphene Oxide-Modified Glassy Carbon Electrode. *ACS Omega*. 2022;7(49):45469-80.

48. Wang R, Liang R, Dai T, Chen J, Shuai X, Liu C. Pectin-based adsorbents for heavy metal ions: A review. *Trends in Food Science & Technology*. 2019;91:319-29.

49. Vytrřas K, Svancara I, Metelka R. Carbon paste electrodes in electroanalytical chemistry. *Journal of the Serbian Chemical Society*. 2009;74(10):1021-33.

50. Allé PH, Fanou GD, Robert D, Adouby K, Drogui P. Photocatalytic degradation of Rhodamine B dye with TiO<sub>2</sub> immobilized on SiC foam using full factorial design. *Applied Water Science*. 2020;10(9).

51. Liang RH, Li Y, Huang L, Wang XD, Hu XX, Liu CM, et al. Pb(2+) adsorption by ethylenediamine-modified pectins and their adsorption mechanisms. *Carbohydr Polym*. 2020;234:115911.

52. Tedesco MP, Garcia VAdS, Borges JG, Osiro D, Vanin FM, Pedroso Yoshida CM, et al. Production of oral films based on pre-gelatinized starch, CMC and HPMC for delivery

of bioactive compounds extract from acerola industrial waste. *Industrial Crops and Products*. 2021;170.

53. Wang S, Wang Z, Huang T, Wang P, Zhang G. Mechanical strengths, drying shrinkage and pore structure of cement mortars with hydroxyethyl methyl cellulose. *Construction and Building Materials*. 2022;314.

54. Larsson M, Johnsson A, Gårdebjer S, Bordes R, Larsson A. Swelling and mass transport properties of nanocellulose-HPMC composite films. *Materials & Design*. 2017;122:414-21.

55. Li D, Jia J, Wang J. A study on the electroanalytical performance of a bismuth film-coated and Nafion-coated glassy carbon electrode in alkaline solutions. *Microchimica Acta*. 2010;169(3-4):221-5.

56. Fonseca W, Ribeiro L, Pradela-Filho L, Takeuchi R, Santos A. Voltammetric Determination of Zn<sup>2+</sup> in Antiseptic Dusting Powder and Multivitamins Using a Carbon Paste Electrode Modified with Bi Anchored on Amberlite® IR120. *Journal of the Brazilian Chemical Society*. 2018.

57. Duay J, Ortiz-Santiago JE, Lambert TN. Copper Sensing in Alkaline Electrolyte Using Anodic Stripping Voltammetry by Means of a Lead Mediator. *Electroanalysis*. 2017;29(12):2685-8.

58. Galus S, Turska A, Lenart A. Sorption and wetting properties of pectin edible films. *Czech Journal of Food Sciences*. 2012;30(5):446-55.

59. Bruno L, Scuderi M, Priolo F, Falcicola L, Mirabella S. Enlightening the bimetallic effect of Au@Pd nanoparticles on Ni oxide nanostructures with enhanced catalytic activity. *Sci Rep*. 2023;13(1):3203.

60. Ning J, Luo X, Wang F, Huang S, Wang J, Liu D, et al. Synergetic Sensing Effect of Sodium Carboxymethyl Cellulose and Bismuth on Cadmium Detection by Differential Pulse Anodic Stripping Voltammetry. *Sensors (Basel)*. 2019;19(24).

61. Niu P, Fernández-Sánchez C, Gich M, Navarro-Hernández C, Fanjul-Bolado P, Roig A. Screen-printed electrodes made of a bismuth nanoparticle porous carbon nanocomposite applied to the determination of heavy metal ions. *Microchimica Acta*. 2015;183(2):617-23.



จุฬาลงกรณ์มหาวิทยาลัย  
**CHULALONGKORN UNIVERSITY**



จุฬาลงกรณ์มหาวิทยาลัย  
**CHULALONGKORN UNIVERSITY**

## VITA

NAME Nuntanuch Lersanantasil  
DATE OF BIRTH 25 January 1999  
PLACE OF BIRTH โรงพยาบาลสุรินทร์  
INSTITUTIONS ATTENDED Chulalongkorn University, B.Sc.  
HOME ADDRESS 564-566 ถ.ชนสาร ต.ในเมือง อ.เมือง จ.สุรินทร์ 32000

